Journal of South American Earth Sciences 31 (2011) 397–413

Contents lists available at ScienceDirect

Journal of South American Earth Sciences

journal homepage: www.elsevier.com/locate/jsames

Geochronology of granulites from the south Itabuna-Salvador-Curaçá Block, São Francisco Craton (Brazil): Nd isotopes and U–Pb zircon ages

Jean-Jacques Peucat [a,*], Johildo Salomão Figueiredo Barbosa [b], Ivana Conceição de Araújo Pinho [b], Jean-Louis Paquette [c], Hervé Martin [c], C. Mark Fanning [d], Angela Beatriz de Menezes Leal [b], Simone Cruz [b]

[a] Géosciences Rennes, UMR CNRS 6118, Université de Rennes-1, 35042 Rennes Cedex, France
[b] UFBA – Universidade Federal da Bahia, CPGG – Centro de Pesquisa em Geofísica e Geologia, Rua Barão de Geremoabo, s/n, Federação, 40170-209 Salvador, Bahia, Brazil
[c] Laboratoire Magmas et Volcans, Département de Géologie, OPGC – Université Blaise Pascal, CNRS – IRD, 5 rue Kessler, 63038 Clermont – Ferrand, France
[d] ANU, Canberra University, Australia

ARTICLE INFO

Article history:
Received 12 October 2010
Accepted 14 March 2011

Keywords:
Nd isotopes
Zircon SHRIMP and LA-ICPMS dating
Archaean and Palaeoproterozoic
Bahia State

ABSTRACT

This work provides five new U–Pb zircon dating and the corresponding Nd isotope data for felsic granulites from the south Itabuna-Salvador-Curaçá Block (ISCB), in the São Francisco Craton, Brazil. Three major sets of felsic granulites can be recognised. The oldest set is tonalitic in composition and of TTG affinity. It is Archaean in age with magmatic zircon cores dated at 2675 ± 11 Ma by LA-ICPMS and up to ca 2.7–2.9 Ga by SHRIMP on an other sample. It exhibits epsilon Nd values between −8 and −11 at 2.1 Ga. This Nd signature is similar to that of granulites found in the western Archaean Jequié Block. Cartographically, this set of Archaean terrains represents at least 50% of the granulites in the studied area. The second set corresponds to a Palaeoproterozoic calc-alkaline tonalitic suite with zircon ages from 2019 ± 19 Ma to 2191 ± 10 Ma and epsilon Nd values between −3 and −4 at 2.1 Ga, corresponding partially to a newly formed crust. The third set of granulites is also Palaeoproterozoic. It is shoshonitic to monzonitic in composition and synchronous with the high grade metamorphism dated by metamorphic zircons at 2086 ± 7 Ma (average of five samples). The Nd isotope signature for this alkaline set is similar to that of the Palaeoproterozoic calc-alkaline one. Nd isotopes appear to be a very efficient tool to distinguish Archaean from Palaeoproterozoic felsic protoliths in granulitic suites of the Itabuna-Salvador-Curaçá Block (ISCB). Finally, the southern part of the ISCB is composed of a mixture of Archaean and Palaeoproterozoic protoliths, in similar amounts, suggesting that it was probably an active margin between 2.1 and 2.2 Ga located on the eastern border of the Archaean Jequié Block. A major crustal thickening process occurred at ca 2.09 Ga in the ISCB and seems significantly younger towards the west, in the Jequié granulites, where an average of 2056 ± 9 Ma is determined for the high grade event.

1. Introduction

Relationships between high grade metamorphism, magmatic accretion and tectonic settings in the lower crust are key issues to understanding the formation of continents: how they grew, were amalgamed and dislocated throughout time. Consequently, it appears important to define the nature and origin of rocks in granulitic terrains and to constrain the timing of magmatic stages and metamorphic event(s) in order to understand such an evolution.

Granulites from the southeastern border of the São Francisco Craton constitute an important reference for the study of the Precambrian lower crust. Tonalitic and trondhjemitic granulites are particularly abundant in the Itabuna-Salvador-Curaçá Block. They have been squeezed between the Archaean Gavião, Jequié and Serrinha blocks (Fig. 1) leading to the formation of an important mountain range, which is now completely eroded away in the centre of the block where the high grade metamorphic rocks are exposed. This forms one of the world's most important granulite provinces (Barbosa, 1986; Barbosa and Sabaté, 2004).

In the current study, we present new U–Pb geochronological and Nd geochemical data for tonalitic and trondhjemitic granulites from the southern part of the ISCB, in conjunction with previously detailed field work and geochemical studies (Barbosa and Sabaté, 2002; Pinho, 2005; Pinho et al., 2011). We determined the timing

* Corresponding author. Tel.: +33 2 23 23 60 85; fax: +33 2 23 23 60 97.
E-mail addresses: peucat@univ-rennes1.fr (J.-J. Peucat), johildo@cpgg.ufba.br (J.S. Figueiredo Barbosa), ivanapinho@yahoo.com.br (I. Conceição de Araújo Pinho), paquette@opgc.univ-bpclermont.fr (J.-L. Paquette), martin@opgc.univ-bpclermont.fr (H. Martin), mark.fanning@anu.edu.au (C.M. Fanning), angelab@ufba.br (A. Beatriz de Menezes Leal), simoneufba@gmail.com (S. Cruz).

0895-9811/$ – see front matter © 2011 Elsevier Ltd. All rights reserved.
doi:10.1016/j.jsames.2011.03.009

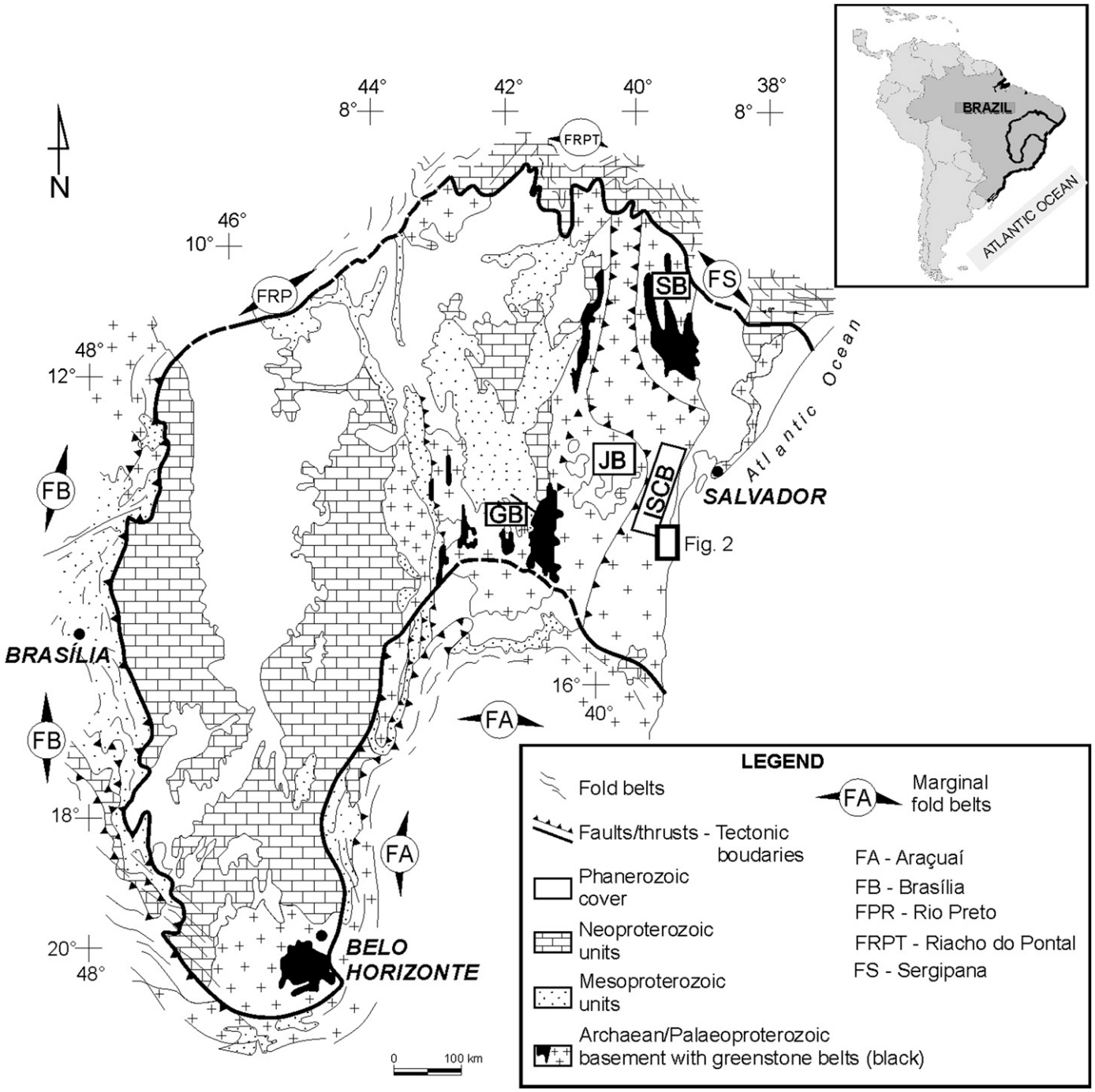

Fig. 1. Schematic geological map showing the limits, marginal fold belts and major structural units of the São Francisco Craton. GB – Gavião Block; JB – Jequié Block; SB – Serrinha Block; ISCB – Itabuna-Salvador-Curaçá Block (adapted from Alkmim et al., 1993). The black rectangle indicates the studied area.

of magmatic protoliths for several tonalitic and trondhjemitic suites as well as the age of the high grade metamorphic event in this part of the ISCB. Finally, we estimate the proportion of Archaean and Palaeoproterozoic magmas in the south ISCB and discuss the geodynamical setting of the ISCB and of the Jequié Block in the São Francisco Craton.

2. Geological setting

The São Francisco Craton, which stabilised during the Palaeoproterozoic, is located in Brazil in the central-eastern part of the South American Plate. In the stable part of the craton, Mesoproterozoic and Neoproterozoic sediments overlie an Archaean-Palaeoproterozoic basement (Alkmim et al., 1993; Teixeira et al., 2000; Fig. 1). In this basement, Barbosa and Sabaté (2004) identified four distinct crustal segments: the Gavião (GB), Jequié (JB), Serrinha (SB) and Itabuna-Salvador-Curaçá (ISCB) blocks (Fig. 1). Geological evidence coupled with structural, metamorphic and available radiometric data is consistent with a collision of these four crustal segments (GB, JB, SB and ISCB) during the Palaeoproterozoic, resulting in the formation of a N–S mountain belt approximately 600 km long and 150 km wide. Evidence of this

collision is not only recorded in the structural features, but also in the pre- and syntectonic Palaeoproterozoic rocks that are intruded into these crustal segments, mainly in the Gavião Block (Marinho, 1991; Santos Pinto et al., 1998; Bastos Leal, 2003), the Itabuna-Salvador-Curaçá Block (Ledru et al., 1994; Barbosa and Sabaté, 2004) and the Serrinha Block (Oliveira et al., 1999, 2002; Melo et al., 2000; Rios et al., 2005, 2008, 2009). During the collision, slices of the Jequié Block may have been incorporated into the Itabuna-Salvador-Curaçá Block.

The Gavião Block (GB) (Fig. 1) is made up of various orthogneisses including TTG suites with ages ranging from 3.5 to 2.7 Ga. They were metamorphosed and partially recycled in migmatites and granites dated at ca 2.7–2.5 Ga (Marinho, 1991; Martin et al., 1991; Nutman and Cordani, 1993; Santos Pinto, 1996; Santos Pinto et al., 1998; Bastos Leal et al., 2003; Peucat et al., 2003). Locally they have been strongly metamorphosed during Palaeoproterozoic events around 2.1 Ga (Santos Pinto et al., 1998). Disrupted supracrustal belts (Marinho, 1991; Cunha and Fróes, 1994; Mascarenhas and Silva, 1994) are Archaean with ages at approximately 3.3 and 2.7 Ga (Peucat et al., 2002; Bastos Leal et al., 2003).

The Jequié Block (JB) (Fig. 1) crops out in between the Gavião Block and Itabuna-Salvador-Curaçá Block. It consists of two main lithologic units. The older one, dated at ca 3.0 Ga by Wilson (1987), is made up of heterogeneous ortho-derived granulites with subordinate mafic facies associated with sedimentary derived granulites including kinzigites, iron formations, orthopyroxene-bearing garnet quartzites and graphitites. The second unit is younger (2.6–2.7 Ga old) and contains enderbitic, charno-enderbitic and charnockitic

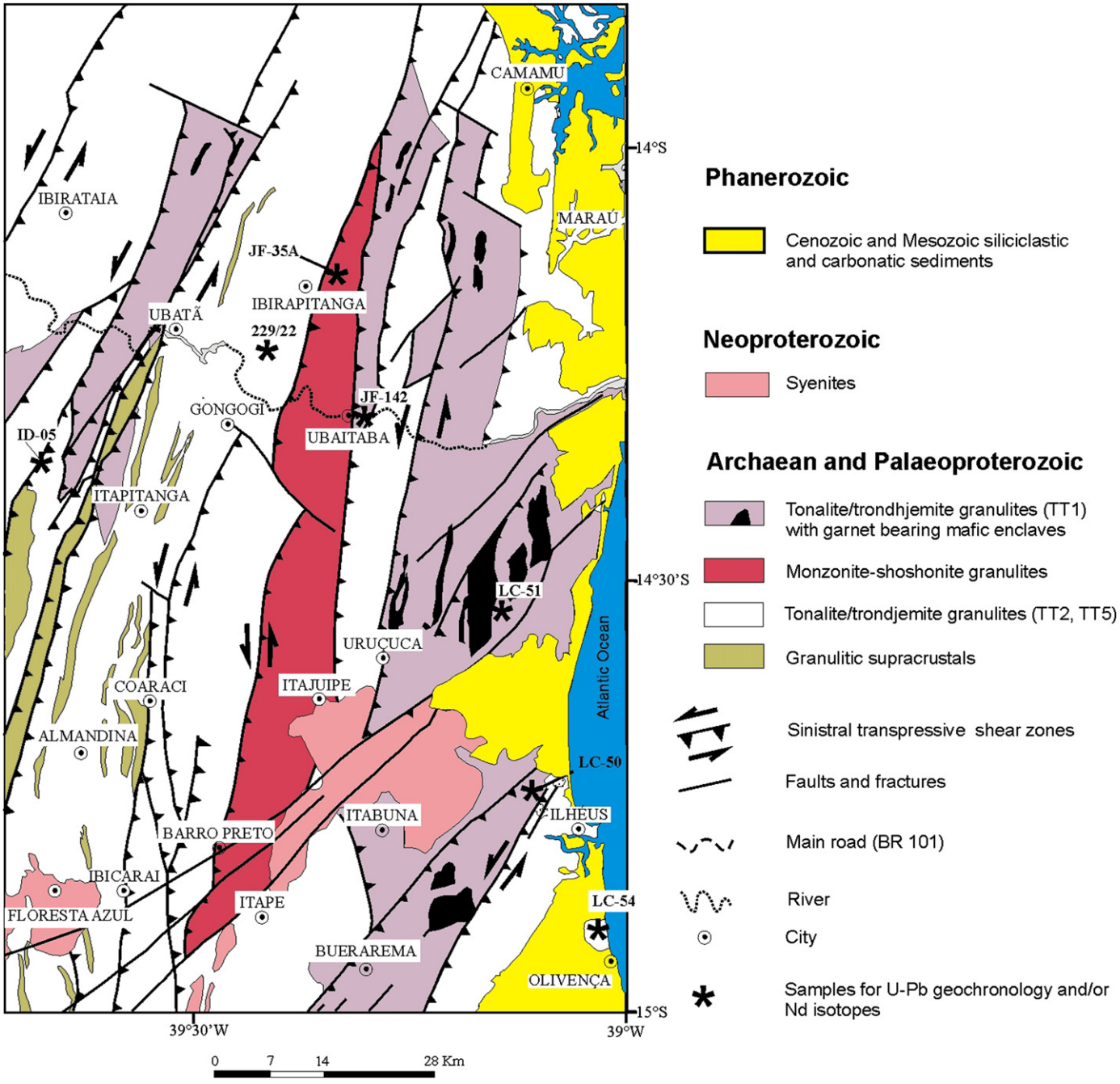

Fig. 2. Simplified geological map of the studied area (modified from Barbosa, 1990). Samples used in this work and those of Silva et al. (2002) are reported.

granulites (Alibert and Barbosa, 1992; Silva et al., 2002; Barbosa et al., 2004).

The Serrinha Block (SB) (Fig. 1) crops out at the north-eastern extremity of the São Francisco Craton. It is composed of tonalitic, granodioritic Archaean orthogneisses whose ages range from 3.1 to 2.8 Ga (Cordani et al., 1999; Oliveira et al., 1999, 2002; Melo et al., 2000; Rios et al., 2005, 2008, 2009). Palaeoproterozoic calc-alkaline plutons were emplaced at ca 2.15 Ga and alkaline suites ca 2.10 Ga, (Rios et al., 2008, 2009). Rios et al., (2008) indicate the occurence of 3.6 Ga zircon xenocrysts in a 2.16 Ga trondhjemite.The 2.15–2.12 Ga old Rio Itapicuru and Rio Capim greenstone belts (Silva, 1996; Oliveira et al., 2011) overlie the basement and are intruded by a wide variety of granites (Alves da Silva, 1994) with ages between 2.10 and 2.07 Ga (Rios et al., 2005, 2008; Oliveira et al., 2011).

The granulitic Itabuna-Salvador-Curaçá Block (ISCB, Figs. 1 and 2) is located between the Gavião and Serrinha blocks in the north and on the eastern side of the Jequié Block in the south. In its northern part, it mainly consists of gneissic suites with imbrications of supracrustal belts with both types dated at ca 2.6–2.7 Ga (Silva et al., 2002; Oliveira et al., 2010). Tonalitic suites were emplaced around 2.25 Ga in the Curaçá belt (D'el-Rey Silva et al., 2007). Some charnockites dated ca 2.1 Ga were also recognised (Silva et al., 2002; Barbosa et al., 2008) and the granulite facies metamorphism is dated around 2.07 Ga (Oliveira et al., 2010).

The southern part of the ISCB (this work) is composed of at least three main groups of granulites including (Fig. 2): (1) meta-sedimentary belts with interlayed mafic rocks; (2) tonalitic-trondhjemitic suites, which are studied in this work (previous U–Pb zircon dating is detailed in Section 3.3 and Table 4) and (3) monzonite-shoshonitic granulites dated around 2.1 Ga (Ledru et al., 1994; Alibert pers. com.). In this area, the granulite facies metamorphism is of high temperature (800–850°C) and medium pressure (7–9 kb), it is dated at ca 2.1 Ga (Ledru et al., 1994; Silva et al., 2002; Barbosa et al., 2008). This granulite facies metamorphism is interpreted as resulting from a collision between the four previously described continental blocks (Barbosa and Sabaté, 2002, 2004).

The tonalitic and trondhjemitic (TT) granulites are the most widespread lithologies in the southern part of the ISCB, where they are associated with monzonite-shoshonitic granulites in the field (Fig. 2). TT granulites mainly consist of a quartz and antipertithic plagioclase association with minor amounts of orthopyroxene, clinopyroxene and opaque minerals. Perthitic K-feldspar is rare and both hornblende and biotite are retrograde minerals. Based on REE patterns, Barbosa and Sabaté (2002) recognized and mapped three types of felsic protoliths (Fig. 2). (1) The north-south dark grey bands in Fig. 2 are mainly formed by the TT1, which constitute a low-K calc-alkaline suite with fractionated REE patterns (La/Yb_N av. = 39) and no Eu anomalies; the original plutonic assemblages were re-equilibrated during granulite facies metamorphim. TT1 could have been derived from the partial melting of mafic sources similar to the tholeiitic enclaves observed in the granulites (Pinho et al., 2011). (2) White zones correspond mainly to TT2 and TT5 granulites, which are undistinguished on Fig. 2 because they are closely imbricated in the field. TT2 have more fractionated REE patterns than TT1 granulites (La/Yb av. = 45) and positive Eu anomalies. TT5 granulites exhibit less fractionated REE patterns (La/Yb av. = 9) and negative Eu anomalies. (3) The monzonitic to shoshonitic granulites constitute another important group of igneous-derived granulites and are reported in Fig. 2 as a N–S hatched band. Large-scale N70° trending vertical faults affect the granulites and represent paths for the intrusion of Neoproterozoic syenites (Fig. 2).

3. Isotope geochemistry and geochronology

3.1. Analytical methods

Whole rock Nd isotopic compositions were measured using a Finnigan Mat 262 mass spectrometer at Géosciences Rennes-CNRS, France, following procedures described by Peucat et al. (1999). Replicate analyses of the AMES Nd standard provide an average $^{143}Nd/^{144}Nd$ value of 0.511896 ± 7. The error of the $^{143}Nd/^{144}Nd$ ratio is 0.0015%. Nd T_{DM} model ages were calculated using ε_{Nd} values of +10 for the present-day depleted mantle, and $^{147}Sm/^{144}Nd = 0.2137$, assuming a linear radiogenic growth for the mantle starting at 4.54 Ga.

Two U–Pb zircon analyses were performed using the SHRIMP II at the Research School of Earth Sciences, ANU, Australia, following the methods given in Williams (1998). Three U–Pb zircons were dated at the Laboratoire Magmas et Volcans, Clermont-Ferrand (France) using an ICPMS Agilent 7500 cs and a Laser-ablation-system Resonetics-Resolution M-50E with a frequency of 5 Hz and energy density of 9 J/cm2 for laser-ablation analyses; spot size was 20 μm (details in Hurai et al., 2010). Zircon 91500 was used as the Standard. Uncertainties for individual analyses (ratios and ages) are given at the 1σ level in Tables 2 and 3. Errors on discordia intercept ages and $^{207}Pb/^{206}Pb$ weighted mean ages are all given at 2σ (for SHRIMP and LA-ICPMS data) and were calculated using the Isoplot programme of Ludwig (2001). All ages were calculated using the decay constants and isotope abundances listed by Steiger and Jäger (1977).

3.2. Nd isotope geochemistry

Nd isotopic compositions were determined for six granulite samples and discussed with four analyses from Marinho et al. (1994) (Table 1, Fig. 3). A first set of samples corresponding to the TT1 (samples JF142A and YJ16) and shoshonitic granulites (samples JF35A, 1263prj12 and CJ13) have slightly negative ε_{Nd} values (−1.7 to −3.3) at 2.1 Ga and similar T_{DM} ages of ca 2.5 Ga. A second set of samples, related in field to TT1 (TD6 and CJ11), have higher $^{143}Sm/^{144}Nd$ ratios than typical TT1 gneisses. They also exhibit slightly negative ε_{Nd} values at 2.1 Ga however the T_{DM} model ages are older (2.7–2.8 Ga). A third set, comprising samples IDO5 and CJ34A (TT2) and sample 229-22 (TT5), exhibit more negative ε_{Nd} values of −7.6 to −11 at 2.1 Ga with older model ages up to 3.0 Ga.

Isotope growth lines for the ten samples are reported in a ε_{Nd} vs time diagram (Fig. 3). Samples from the first and second sets are above the isotopic evolution field of the Jequié granulites, which consequently exhibit a more negative range of ε_{Nd} values (from −5 to −15) at 2.1 Ga, whilst the third set, with more negative ε_{Nd} values, falls at 2.1 Ga within this field. These results indicate that both the tonalitic (TT1 ss) and shoshonitic granulites contain no or only a limited amount of older crustal components. In other words, they have more juvenile sources than TT2 and TT5 granulites, which involved significant amounts of Archaean material, similar to that of the Jequié granulites. However samples TD6 and CJ11, which also have slightly negative epsilon Nd values at 2.1 Ga but model ages around 2.7–2.8 Ga, could possibly have an older crustal component in their source. In-situ U–Pb dating of both the magmatic protoliths and high grade metamorphic event have been performed using SHRIMP and LA-ICPMS techniques.

3.3. Previous U–Pb dating

Fig. 2 shows the location where the first SHRIMP zircon ages were obtained by Silva et al. (2002) on a charno-enderbite (LC50) located approximately 10 km NW of Ilhéus, an enderbite (LC-51) around 30 km NNE of Ilhéus, and a charnockite (LC 54) from approximatively

Table 1
Sm-Nd isotope data for some granulites of the southern ISCB.

Samples	Sm (ppm)	Nd (ppm)	147Sm/144Nd	143Nd/144Nd	Error 10^{-6} (±2 σm)	εNd (t = 0 Ga)	TDM in Ma (DM_0 = +10)	εNd(t) 2.1 Ga
TT1 granulites:								
JF-142A	1.71	12.83	0.0806	0.510887	5	−34	2578	−3.1
YJ 16	3.30	25.06	0.0794	0.510917	4	−34	2521	−2.1
TD6	2.61	12.10	0.1304	0.511600	5	−20	2819	−2.5
TD 6 dupl.	2.59	11.84	0.1320	0.511650	3	−19	2782	−2.0
CJ11[a]	4.57	23.8	0.1170	0.511403	–	−24	2738	−2.8
Shoshonitic granulites:								
JF35A	1.77	15.55	0.0689	0.510711	8	−38	2553	−3.3
1263pjr12[a]	13.87	90.9	0.0923	0.511094	–	−30	2568	−2.1
CJ13[a]	20.0	150	0.0813	0.510965	–	−33	2503	−1.7
TT2-TT5 granulites:								
ID05	1.86	10.79	0.1043	0.510981	7	−32	3001	−7.6
CJ34a[a]	0.56	4.74	0.0724	0.510370	–	−44	2979	−10.9
229-22	1.60	12.35	0.0784	0.510595	6	−40	2860	−8.1

[a] In Marinho et al. (1994).

20 km SSE of Ilhéus. Samples LC-50 and LC-51 belong to the TT1 group whereas LC-54 belongs to the TT2-TT5 group. LC-50 and LC-51 respectively provide ages of 2092 ± 6 Ma and 2131 ± 5 Ma, which are interpreted as the emplacement age for syn-collisional magmatic protoliths. In sample LC51, metamorphic overgrowths give an age of 2069 ± 19 Ma, which is interpreted as that of the granulite facies metamorphism. LC 54 provides an Archaean age of 2719 ± 10 Ma interpreted in terms of the magmatic cristallisation age. On the other hand, as a TIMS evaporation zircon age of 2075 ± 16 Ma (±2σ) was obtained on a shoshonitic granulite (Ledru et al., 1994) in this country, we interpreted this age as being a minimum age for the magmatic alkaline protolith of these shoshonitic granulites. A summary of the available U–Pb dating from the ISCB and Jequié granulites is given in Table 4 (see discussion).

3.4. New U–Pb zircon dating

U–Pb dating was performed on separate zircons from five granulitic samples: JF-142A and YJ 16 (TT1) with Nd model ages at ca 2.5 Ga; TD6 is also a TT1 granulite but has a model age around 2.7 Ga and finally ID05 (TT2) and 229-22 (TT5), which are the two samples having the oldest model ages (up to 3.0 Ga). SHRIMP and LA-ICPMS U–Pb results are presented in Tables 2 and 3 respectively.

3.4.1. Zircon JF-142A (TT1)

Zircons from JF-142A mainly consist of elongated grains with rounded tips. They have a complex structure with brown cores and clear overgrowths (Figs. 4 and 5). The cores and overgrowths are dated by SHRIMP at 2191 ± 10 Ma and 2109 ± 17 Ma respectively. In more detail, the cores exhibit concentric zoning (Fig. 4) and have high-U content (average = 586 ppm, Table 2): they are interpreted as magmatic grains. $^{207}Pb/^{206}Pb$ ages for the cores range between 2.1 and 2.2 Ga; the oldest concordant core (9.1) provides a $^{207}Pb/^{206}Pb$ age of 2184 ± 11 Ma (Table 2). Four other cores, which are more or less discordant (90–97% of concordancy), give $^{207}Pb/^{206}Pb$ ages that range between 2213 ± 11 Ma (5.2) and 2119 ± 10 Ma (7.1). The average of the three $^{207}Pb/^{206}Pb$ oldest ages is 2191 ± 10 Ma (MSWD = 2.4). This age, ca 2.2 Ga, is interpreted as that of the tonalitic precursor. whereas the ca 2.10 Ga age accounts rather for lead loss processes during the high grade metamorphism (see below).

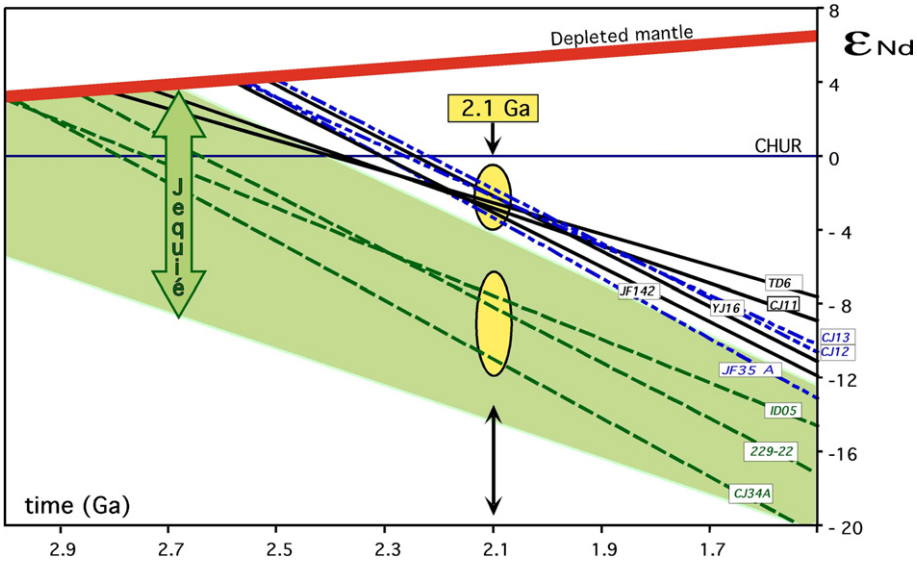

Fig. 3. Nd vs time isotopic evolution diagram for the various sets of granulites in the ISCB. The field for the Archaean Jequié granulites is reported in green (or dark) colour. Ellipses correspond to the range of values observed for epsilon Nd at 2.1 Ga for Palaeoproterozoic precursors (upper ellipse) and Archaean precursors (lower ellipse). (For interpretation of the references to colour in this figure legend, the reader is referred to the web version of this article.)

Table 2
Summary of SHRIMP U–Pb zircon results for samples JF142-A & 229-22.

Grain spot	U (ppm)	Th (ppm)	Th/U	^{206}Pb (ppm)	f_{206} %	Radiogenic Ratios							ρ	Ages (Ma)				% Conc.
						^{204}Pb/^{206}Pb	^{206}Pb/^{238}U	±	^{207}Pb/^{235}U	±	^{207}Pb/^{206}Pb	±		^{206}Pb/^{238}U	±	^{207}Pb/^{206}Pb	±	
JF142-A (TT1)																		
Cores																		
2.1	454	75	0.17	149	0.20	0.00014	0.3802	0.0058	6.942	0.127	0.1324	0.0013	0.837	2077	27	2131	18	97
3.2	360	233	0.65	120	1.61	0.00107	0.3831	0.0051	6.761	0.177	0.1280	0.0029	0.506	2091	24	2070	40	101
5.2	620	278	0.45	212	0.35	0.00024	0.3956	0.0046	7.573	0.102	0.1388	0.0009	0.874	2149	21	2213	11	97
7.1	604	275	0.46	180	0.15	0.00010	0.3460	0.0041	6.276	0.083	0.1315	0.0008	0.897	1916	20	2119	10	90
9.1	932	77	0.08	327	0.13	0.00009	0.4083	0.0047	7.686	0.093	0.1365	0.0006	0.942	2207	21	2184	7	101
10.1	549	187	0.34	182	0.30	0.00020	0.3852	0.0045	7.275	0.097	0.1370	0.0008	0.888	2101	21	2189	11	96
Overgrowths																		
1.2	187	155	0.83	63	0.95	0.00064	0.3887	0.0077	7.005	0.191	0.1307	0.0024	0.728	2117	36	2108	33	100
2.2	165	69	0.42	51	0.87	0.00059	0.3611	0.0054	6.527	0.164	0.1311	0.0027	0.590	1987	25	2113	36	94
4.1	349	366	1.05	110	0.37	0.00025	0.3668	0.0047	6.519	0.104	0.1289	0.0012	0.798	2014	22	2083	17	97
5.1	170	157	0.92	58	1.08	0.00072	0.3932	0.0055	7.073	0.161	0.1305	0.0023	0.615	2138	25	2104	31	102
6.1	147	55	0.37	48	1.07	0.00071	0.3721	0.0064	6.289	0.166	0.1226	0.0025	0.648	2039	30	1994	36	102
7.2	122	68	0.56	38	1.31	0.00088	0.3567	0.0053	6.438	0.208	0.1309	0.0038	0.459	1966	25	2110	50	93
8.1	243	63	0.26	78	0.81	0.00054	0.3710	0.0050	6.730	0.129	0.1316	0.0018	0.705	2034	24	2119	24	96
9.2	101	55	0.55	33	0.84	0.00056	0.3753	0.0057	6.875	0.165	0.1329	0.0025	0.631	2054	27	2136	33	96
11.1	176	228	1.30	60	0.60	0.00041	0.3929	0.0053	7.230	0.134	0.1335	0.0017	0.731	2136	25	2144	22	100
11.2	163	241	1.48	54	1.20	0.00080	0.3769	0.0058	6.722	0.168	0.1294	0.0025	0.620	2062	27	2089	34	99
Ext. rim 1.1	75	29	0.39	24	1.95	0.00131	0.3743	0.0076	6.803	0.313	0.1318	0.0054	0.442	2050	36	2122	72	97
Ext. rim 2.3	57	24	0.42	19	2.38	0.00159	0.3794	0.0078	6.719	0.367	0.1284	0.0065	0.376	2073	36	2077	89	100
Ext. rim 3.1	79	23	0.29	26	2.32	0.00154	0.3789	0.0069	6.660	0.302	0.1275	0.0053	0.405	2071	32	2064	73	100
Ext. rim 4.2	89	12	0.14	27	0.92	0.00062	0.3537	0.0058	6.572	0.191	0.1348	0.0032	0.570	1952	28	2161	42	90
229-22 (TT5)																		
Cores																		
1.2	627	164	0.26	118	0.001	0.00010	0.4704	0.0071	11.018	0.247	0.1654	0.0021	0.753	2485	31	2556	25	97
3.1	168	177	1.05	42	0.004	0.00025	0.5266	0.0093	12.884	0.374	0.1906	0.0036	0.701	2727	40	2629	35	104
3.2	187	83	0.44	41	0.003	0.00023	0.5182	0.0103	13.325	0.309	0.1749	0.0018	0.910	2691	44	2712	16	99
5.1	1317	158	0.12	239	0.001	0.00004	0.4791	0.0060	9.731	0.172	0.1522	0.0014	0.790	2523	26	2315	19	109
5.2	813	163	0.20	140	0.002	0.00013	0.4428	0.0067	9.166	0.202	0.1492	0.0015	0.767	2363	30	2347	25	101
6.1	550	219	0.40	102	0.002	0.00015	0.4536	0.0069	9.612	0.176	0.1632	0.0025	0.885	2411	31	2387	15	101
6.2	633	212	0.34	107	0.003	0.00021	0.4198	0.0095	9.024	0.314	0.1535	0.0018	0.736	2260	43	2412	41	94
7.2	2231	158	0.07	318	0.001	0.00008	0.3852	0.0045	6.903	0.087	0.1301	0.0004	0.959	2101	21	2097	6	100
8.1	1938	265	0.14	315	0.000	0.00003	0.4264	0.0048	8.683	0.123	0.1457	0.0015	0.866	2290	22	2319	12	99
8.2	644	323	0.50	125	0.002	0.00015	0.4575	0.0066	10.818	0.211	0.1601	0.0032	0.816	2428	29	2572	19	94
11.2	473	172	0.36	248	0.002	0.00012	0.5730	0.0091	16.229	0.294	0.2007	0.0030	0.924	2920	37	2870	11	102
12.2	275	93	0.34	120	0.015	0.00110	0.4897	0.0093	12.184	0.334	0.1797	0.0036	0.773	2569	40	2657	29	97
13.1	1003	61	0.06	358	0.001	0.00007	0.4354	0.0067	9.239	0.182	0.1548	0.0013	0.851	2330	30	2390	18	98
14.1	616	203	0.33	238	0.002	0.00010	0.4406	0.0085	9.478	0.309	0.1558	0.0020	0.683	2354	38	2413	41	98
14.2	1337	106	0.08	472	0.001	0.00007	0.4339	0.0052	8.487	0.120	0.1431	0.0008	0.900	2323	23	2250	11	103
16.1	61	30	0.50	29	0.012	0.00083	0.5248	0.0180	12.243	0.676	0.1645	0.0082	0.711	2720	77	2550	67	107
Overgrowths																		
1.1	23	87	3.77	6	0.036	0.00241	0.4012	0.0155	6.785	0.544	0.1410	0.0037	0.584	2175	72	1995	121	109
4.1	84	288	3.44	23	0.015	0.00098	0.4348	0.0129	8.050	0.344	0.1334	0.0039	0.775	2327	58	2155	48	108
4.2	286	134	0.47	46	0.002	0.00015	0.3912	0.0053	6.990	0.113	0.1293	0.0011	0.893	2128	25	2093	13	102
7.1	204	29	0.14	30	0.007	0.00044	0.3901	0.0072	6.964	0.206	0.1308	0.0013	0.714	2124	34	2091	37	102
9.1	20	160	7.82	9	0.052	0.00347	0.3919	0.0148	6.828	0.597	0.1220	0.0126	0.540	2132	69	2048	137	104
10.1	39	105	2.67	10	0.022	0.00150	0.4054	0.0116	7.023	0.379	0.1245	0.0060	0.629	2194	53	2038	77	108
11.1	35	120	3.46	19	0.008	0.00056	0.3567	0.0153	6.396	0.431	0.1303	0.0047	0.723	1967	73	2098	85	94
12.1	507	93	0.18	184	0.000	0.00002	0.4349	0.0107	8.202	0.273	0.1428	0.0027	0.811	2328	48	2187	35	107
15.1	42	37	0.88	16	0.025	0.00169	0.3834	0.0115	6.563	0.423	0.1243	0.0079	0.568	2092	54	2017	98	104
16.2	24	215	9.12	25	0.009	0.00066	0.3982	0.0193	8.139	0.543	0.1455	0.0074	0.800	2161	89	2326	71	93

Notes : 1. Uncertainties given at the one σ level. 2. f_{206} % denotes the percentage of ^{206}Pb that is common Pb. 3. Correction for common Pb made using the measured ^{204}Pb/^{206}Pb ratio. 4. For % Conc., 100% denotes a concordant analysis.

Table 3
Summary of LA-ICPMS U–Pb zircon results for samples YJ16, TD6 and ID05.

Grain spot	U (ppm)	Th (ppm)	Pb (ppm)	Th/U	Radiogenic ratios				ρ	Ages (Ma)						% Conc.
					$^{207}Pb/^{235}U$	±	$^{206}Pb/^{238}U$	±		$^{206}Pb/^{238}U$	±	$^{207}Pb/^{235}U$	±	$^{207}Pb/^{206}Pb$	±	
YJ16 (TT1)																
Cores																
1.1	1096	342	411	0.31	7.001	0.087	0.3863	0.0039	0.81	2113	19	2115	13	2113	19	100
2.1	1039	662	413	0.64	6.763	0.087	0.3743	0.0038	0.79	2114	19	2113	13	2098	19	101
3.1	3139	266	1173	0.08	6.443	0.079	0.3687	0.0037	0.83	2051	18	2051	13	2045	19	100
4.1	3915	420	1253	0.11	5.880	0.074	0.3437	0.0035	0.81	2042	18	2040	13	2030	19	101
5.1	3428	362	1175	0.11	6.499	0.080	0.3702	0.0038	0.83	2033	18	2044	13	2046	19	99
6.1	4159	567	1699	0.14	6.439	0.079	0.3675	0.0037	0.83	2047	18	2049	13	2035	19	101
7.1	3570	503	1187	0.14	6.460	0.080	0.3665	0.0037	0.82	2066	18	2065	14	2056	19	101
8.1	4551	441	1569	0.10	6.330	0.078	0.3632	0.0037	0.83	2040	18	2043	14	2034	19	100
9.1	911	159	333	0.17	6.585	0.085	0.3640	0.0037	0.79	2096	19	2104	15	2108	19	99
10.1	5140	632	1695	0.12	6.008	0.075	0.3436	0.0035	0.81	2060	18	2060	15	2038	19	101
11.1	4038	385	1374	0.10	6.481	0.080	0.3706	0.0038	0.82	2060	18	2059	15	2037	19	101
12.1	3009	531	1012	0.18	6.468	0.081	0.3696	0.0037	0.81	2055	18	2054	16	2040	19	101
13.1	2590	349	999	0.13	6.621	0.084	0.3719	0.0038	0.80	2068	19	2074	16	2062	19	100
13.2	3859	538	1377	0.14	6.463	0.081	0.3691	0.0037	0.80	2057	19	2055	16	2037	19	101
14.1	2365	292	771	0.12	6.738	0.086	0.3757	0.0038	0.79	2103	19	2100	17	2076	19	101
15.1	1115	263	373	0.24	6.754	0.088	0.3693	0.0037	0.78	2087	19	2109	18	2118	19	99
16.1	1431	216	553	0.15	6.626	0.085	0.3753	0.0038	0.79	2069	19	2068	18	2058	19	101
Metamorphic grains																
17.1	128	192	59	1.50	6.122	0.110	0.3569	0.0037	0.58	2041	19	2035	21	2056	21	99
20.1	237	231	94	0.97	6.728	0.102	0.3788	0.0039	0.67	2078	19	2079	21	2094	20	99
Overgrowths																
18.1	438	205	144	0.47	6.458	0.091	0.3639	0.0037	0.72	2081	19	2080	20	2084	20	100
19.1	154	194	65	1.26	6.611	0.106	0.3734	0.0038	0.64	2071	19	2076	21	2083	20	99
21.1	349	214	126	0.61	6.710	0.096	0.3768	0.0038	0.71	2070	19	2077	21	2079	20	100
22.1	355	299	136	0.84	6.522	0.095	0.3732	0.0038	0.70	2056	19	2055	22	2065	20	100
22.2	305	270	119	0.89	6.789	0.100	0.3798	0.0039	0.69	2086	20	2088	22	2084	20	100
TD6 (TT1 rel.)																
Cores																
1.1	1587	221	535	0.14	7.050	0.096	0.3777	0.0038	0.75	2133	20	2152	24	2137	20	100
1.2	598	244	210	0.41	7.445	0.112	0.3974	0.0040	0.67	2163	21	2167	25	2178	20	99
2.1	2595	584	1034	0.22	6.400	0.086	0.3620	0.0037	0.75	1973	19	2025	24	2051	20	96
3.1	1949	122	596	0.06	6.442	0.088	0.3635	0.0037	0.73	1988	19	2033	25	2061	20	96
4.1	2767	102	940	0.04	6.392	0.087	0.3685	0.0037	0.74	2047	20	2044	25	2024	20	101
7.1	3250	144	1101	0.04	6.629	0.093	0.3757	0.0038	0.72	2060	21	2065	29	2039	20	101
8.1	1592	59	491	0.04	6.611	0.097	0.3688	0.0037	0.69	1843	19	1963	30	2065	20	89
9.1	1498	143	504	0.10	6.542	0.094	0.3656	0.0037	0.70	2087	22	2093	31	2068	20	101
11.1	3507	249	1185	0.07	6.343	0.092	0.3543	0.0036	0.69	2059	22	2066	33	2056	21	100
12.1	1216	380	432	0.31	6.285	0.095	0.3328	0.0034	0.67	1957	21	2064	33	2150	21	91
14.1	1960	60	548	0.03	5.956	0.093	0.3309	0.0034	0.65	1873	21	1983	36	2076	21	90
14.2	2870	162	972	0.06	6.539	0.098	0.3663	0.0037	0.67	2085	23	2090	37	2064	21	101
15.1	1999	103	733	0.05	6.277	0.095	0.3559	0.0036	0.67	2045	23	2058	38	2044	21	100
18.1	1770	110	525	0.06	6.312	0.098	0.3576	0.0036	0.65	1944	23	2009	40	2046	21	95
20.1	1958	100	658	0.05	6.315	0.099	0.3577	0.0036	0.65	2027	24	2051	42	2042	22	99
21.1	2425	116	792	0.05	6.432	0.102	0.3648	0.0037	0.64	2067	25	2072	45	2035	22	102
24.1	850	216	297	0.25	6.571	0.109	0.3693	0.0038	0.61	2087	26	2087	47	2069	22	101
Overgrowths																
4.2	34	4	10	0.11	6.244	0.168	0.3595	0.0039	0.41	2056	21	2068	32	2071	25	99
6.1	36	12	12	0.34	5.856	0.152	0.3450	0.0038	0.42	2069	21	2073	31	2073	25	100
7.2	103	27	35	0.27	6.866	0.118	0.3797	0.0039	0.60	2043	21	2075	31	2105	21	97
24.2	92	16	30	0.17	6.791	0.134	0.3796	0.0039	0.52	2067	27	2085	49	2100	23	98
TD6 (TT1 rel.)																
Metamorphic grains																
5.1	176	134	65	0.76	6.411	0.103	0.3685	0.0038	0.64	2024	20	2044	27	2064	21	98
10.1	169	40	55	0.24	6.668	0.117	0.3754	0.0039	0.58	2060	22	2070	33	2067	22	100
13.1	73	13	23	0.18	6.587	0.143	0.3724	0.0039	0.48	2053	23	2062	36	2069	23	99
16.1	68	12	26	0.18	6.191	0.147	0.3593	0.0038	0.45	2034	24	2038	41	2047	25	99
17.1	114	41	39	0.36	6.737	0.122	0.3773	0.0039	0.57	2049	24	2052	40	2098	22	98
19.1	79	15	27	0.19	6.768	0.145	0.3778	0.0040	0.49	2065	25	2080	43	2076	24	99
22.1	46	5	15	0.11	6.492	0.153	0.3670	0.0039	0.45	2053	26	2078	48	2092	25	98
23.1	81	45	29	0.56	6.438	0.135	0.3710	0.0039	0.50	2049	26	2049	47	2065	24	99
25.1	288	216	113	0.75	6.482	0.118	0.3662	0.0038	0.56	2048	27	2059	49	2066	23	99
26.1	97	17	33	0.18	6.697	0.146	0.3747	0.0039	0.48	2054	27	2071	51	2064	24	100
27.1	126	49	43	0.39	6.540	0.129	0.3719	0.0039	0.52	2050	27	2057	52	2068	23	99

(*continued on next page*)

Table 3 (*continued*)

Grain spot	U (ppm)	Th (ppm)	Pb (ppm)	Th/U	Radiogenic ratios				ρ	Ages (Ma)						% Conc.
					$^{207}Pb/^{235}U$	±	$^{206}Pb/^{238}U$	±		$^{206}Pb/^{238}U$	±	$^{207}Pb/^{235}U$	±	$^{207}Pb/^{206}Pb$	±	
ID05 (TT2)																
Cores																
1.1	385	211	178	0.55	11.519	0.178	0.48157	0.00484	0.65	2526	21	2554	15	2584	20	98
2.1	103	90	52	0.88	12.439	0.226	0.48917	0.00498	0.56	2589	22	2634	18	2675	20	97
3.1	145	65	65	0.45	12.304	0.228	0.49214	0.00502	0.55	2521	21	2592	18	2679	20	94
4.1	169	70	81	0.42	13.286	0.226	0.51460	0.00521	0.59	2687	22	2705	17	2702	20	99
6.1	155	122	69	0.78	11.027	0.242	0.44140	0.00460	0.47	2367	21	2541	21	2666	21	89
7.1	275	231	142	0.84	12.417	0.206	0.48785	0.00492	0.61	2600	22	2661	18	2689	20	97
9.1	180	98	89	0.54	12.786	0.224	0.51029	0.00516	0.58	2654	23	2670	20	2676	20	99
10.1	616	435	283	0.71	11.345	0.190	0.45565	0.00460	0.60	2529	22	2622	20	2650	20	95
11.1	160	118	80	0.74	11.440	0.210	0.47338	0.00481	0.55	2567	22	2604	22	2623	21	98
11.2	152	89	73	0.59	12.419	0.228	0.49701	0.00505	0.55	2601	23	2643	23	2673	21	97
12.1	140	123	67	0.88	10.511	0.215	0.45550	0.00469	0.50	2548	22	2561	24	2555	21	100
13.1	153	96	72	0.63	11.470	0.238	0.45460	0.00468	0.50	2514	22	2605	24	2656	21	95
14.1	123	88	58	0.72	10.566	0.240	0.43714	0.00456	0.46	2468	22	2555	25	2577	22	96
15.1	239	115	104	0.48	11.936	0.212	0.47722	0.00483	0.57	2461	22	2585	25	2660	21	93
16.1	68	43	31	0.63	11.685	0.280	0.46543	0.00487	0.44	2422	23	2568	31	2680	22	90
18.1	146	72	64	0.50	11.159	0.263	0.44073	0.00462	0.44	2450	23	2596	32	2658	22	92
19.1	100	69	51	0.69	12.908	0.268	0.51212	0.00525	0.49	2655	25	2682	33	2679	21	99
20.1	96	60	49	0.62	13.606	0.283	0.51500	0.00528	0.49	2579	25	2701	34	2713	21	95
21.1	125	73	60	0.59	11.682	0.235	0.49007	0.00502	0.51	2542	25	2585	33	2606	22	98
22.1	166	123	86	0.74	12.886	0.249	0.51345	0.00523	0.53	2612	25	2668	34	2663	21	98
Metamorphic grains																
5.1	1979	107	621	0.05	6.840	0.101	0.37451	0.00375	0.68	2045	18	2084	15	2090	21	98
8.1	2134	244	619	0.11	5.858	0.090	0.32418	0.00325	0.65	1995	17	2061	16	2071	21	96
17.1	183	266	80	1.46	6.594	0.122	0.37562	0.00382	0.55	2063	20	2073	27	2073	23	99
17.2	132	126	51	0.96	6.746	0.130	0.37561	0.00384	0.53	2009	19	2076	28	2087	23	96

Notes : 1. Uncertainties given at the one σ level. 2. For % Conc., 100% denotes a concordant analysis.

The overgrowths display irregular or restricted zoning and they have low-U contents (average = 151 ppm) when compared to the cores (586 ppm). In some grains, low-U overgrowths are strongly developed (gr.1 and gr.4, Fig. 5). At least two stages of overgrowths are observed in these grains, (i.e. gr.1), the most internal of which is low in U (101–170 ppm) while the outer one is more U-depleted (57–79 ppm). Both low-U overgrowth types are interpreted as having developed during the high grade metamorphism. Because the data are concordant to slightly discordant (≥90% of concordancy, Fig. 5, Table 2), the mean $^{207}Pb/^{206}Pb$ age of 2109 ± 17 Ma (14 analyses, 6.1 rejected, MSWD = 0.7) is considered as the most significant and is interpreted as the age of the granulite facies metamorphism.

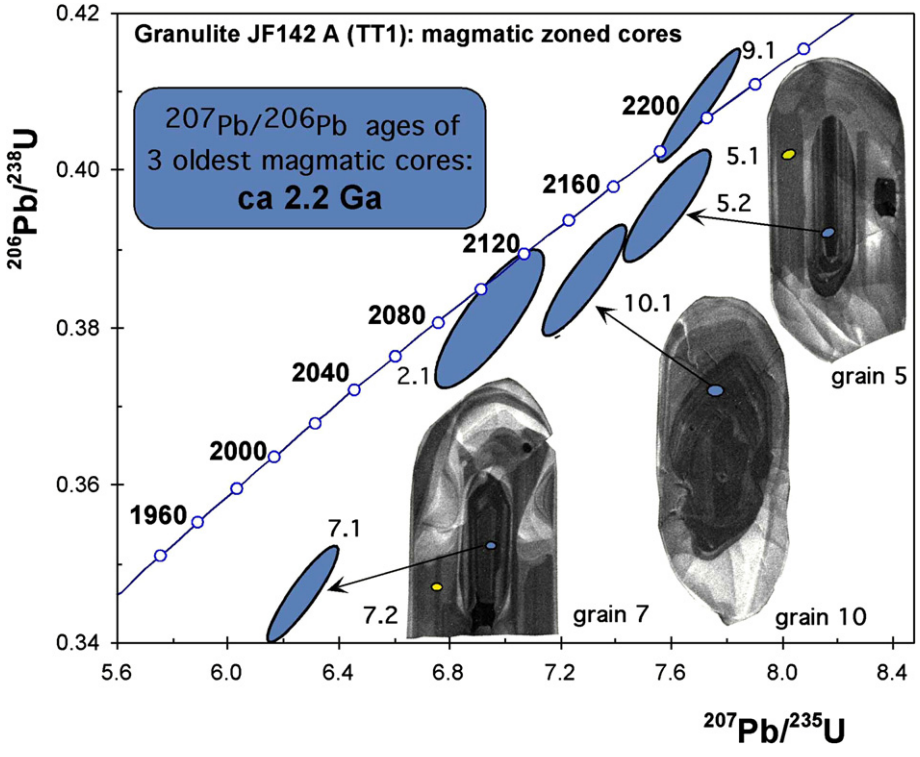

Fig. 4. Concordia diagram and cathodo-luminescence images (CL) for magmatic zircons from granulite JF-142A (TT1). SHRIMP analyses, ellipses are reported at 1σ. Spot size: 30 μm.

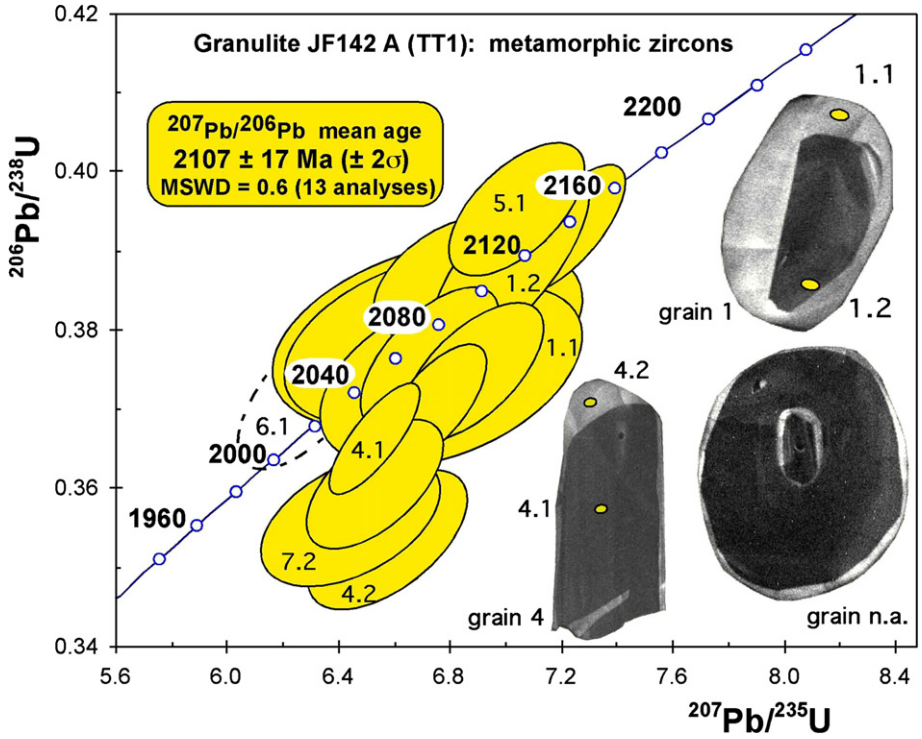

Fig. 5. Concordia diagram and CL images for metamorphic zircons from granulite JF-142A (TT1). SHRIMP analyses, ellipses are reported at 1σ. Spot size 30 μm.

3.4.2. Zircon YJ16 (TT1)

Zircons from sample YJ16 are mainly sub-euhedral, elongate and brown. They are strongly zoned (gr. 2 and 12, Fig. 6) and are interpreted as magmatic grains, dated by LA-ICPMS at 2109 ± 19 Ma. Some of these zoned grains are surrounded by clear unzoned metamorphic overgrowths (gr. 12, 18 and 21, Fig. 7), which were dated at 2081 ± 16 Ma. In more detail, the magmatic zircons are U-Th rich (the U content average of the 18 analyses is around 2900 ppm, Table 3). Overgrowths are U-depleted (average of 7 analyses: 281 ppm). The two data sets are concordant to slightly discordant and give similar ages (both sets define a single intercept at 2110 ± 35 Ma, MSWD = 2.2). The U-rich cores alone (Fig. 6) define an intercept at 2117 ± 49 Ma (MSWD = 2.9) whereas the $^{207}Pb/^{206}Pb$ ages range between 2030 ± 19 Ma and 2118 ± 19 Ma. Considering the

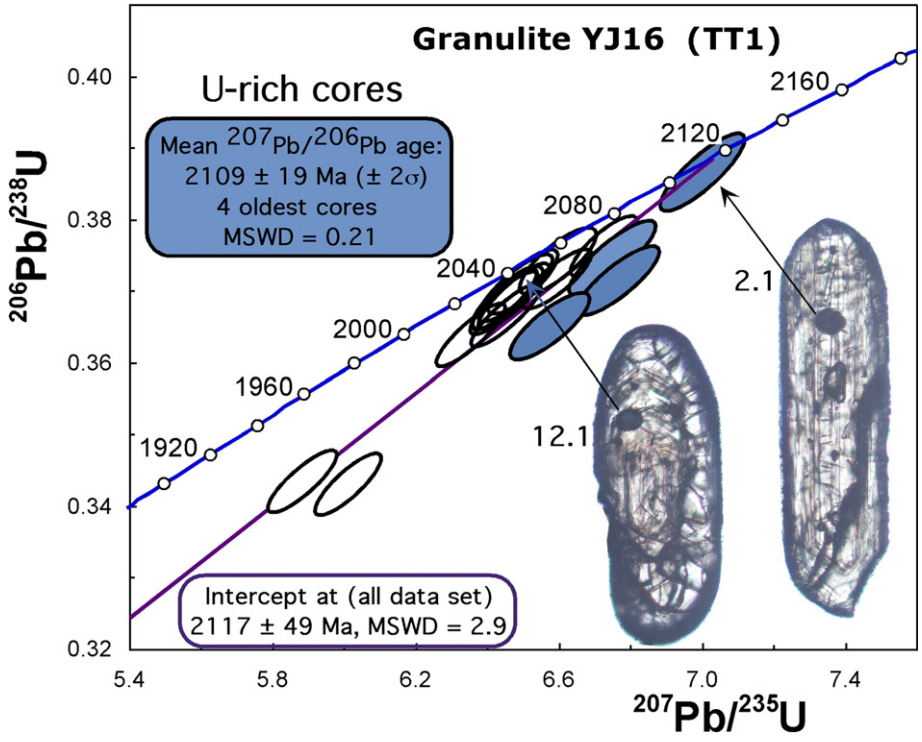

Fig. 6. Concordia diagram and transmitted light images (TL) for magmatic zircons from granulite YJ16 (TT1). LA-ICPMS analyses, ellipses are reported at 1σ. Spot size: 20 μm.

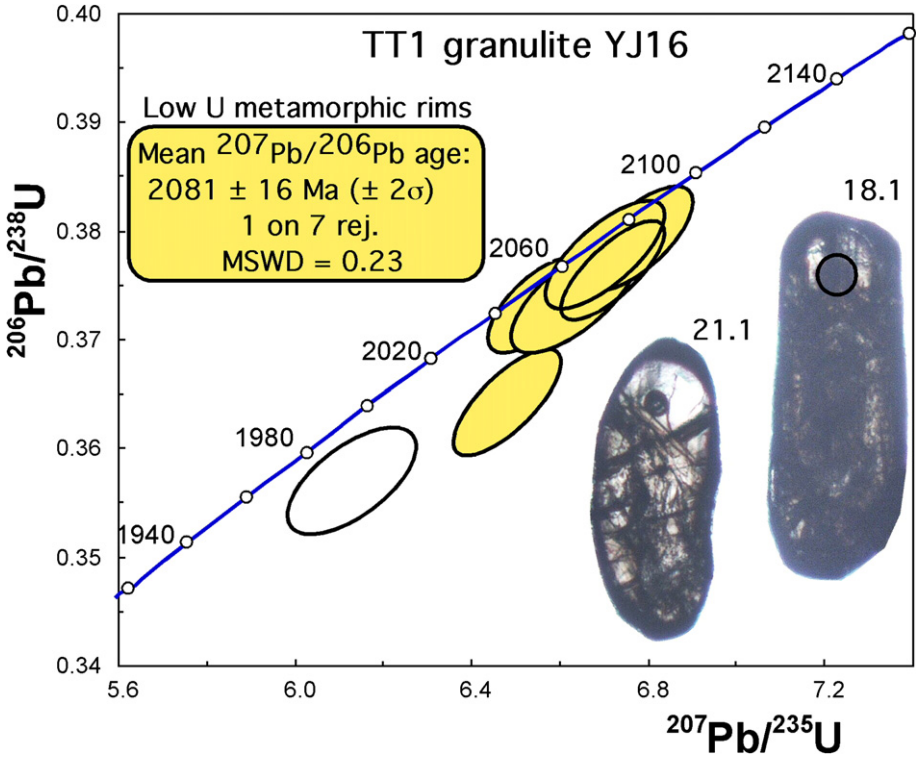

Fig. 7. Concordia diagram and TL images for metamorphic zircons from granulite YJ16 (TT1). LA-ICPMS analyses, ellipses are reported at 1σ. Spot size: 20 μm.

youngest set of ages as probably having been reset during or after the high grade event, we interpret the average of the $^{207}Pb/^{206}Pb$ ages obtained from the four oldest cores at 2109 ± 19 Ma (MSWD = 0.21) as the more realistic age for the magmatic precursor of this granulite. The U-depleted overgrowths are also concordant (Fig. 7, Table 3). The average of $^{207}Pb/^{206}Pb$ ages for 6 out of 7 concordant points (spot 17.1 rejected) is 2081 ± 16 Ma (MSWD = 0.23). It is interpreted as the age of the high grade metamorphism.

3.4.3. Zircon TD6 (TT1 related)

Zircons from sample TD6 correspond to a first set of elongate grains with strongly zoned brown cores and rounded tips corresponding to clear overgrowths (gr. 1, 11 and 21, Fig. 8). A second set of round clear grains, either with or without cores, is also well developed (gr. 17 and 26, Fig. 9). The zoned cores are interpreted as magmatic zircons and were not precisely dated up to ca 2.18 Ga by LA-ICPMC. Overgrowths and round grains are interpreted as metamorphic zircons and provide an age of 2078 ± 13 Ma. In more detail, the zoned cores are U-Th rich (the U average is around 2000 ppm, Table 3) whereas overgrowths and round clear grains are U-depleted (100 ppm). In the concordia diagram (Fig. 8), the $^{207}Pb/^{206}Pb$ ages of cores scatter between 2.02 Ga and 2.18 Ga. The 15 most concordant cores define an imprecise intercept at 2187 ± 99 Ma and the oldest concordant grain (spot 1.2) is ca 2.18 Ga old. We consider the age of the magmatic precursor as being around 2.2 Ga without any evidence for relicts of Archaean zircons. Overgrowths and round grains are concordant to sub-concordant (Fig. 9) in the U–Pb diagram, the $^{207}Pb/^{206}Pb$ ages range from 2.05 to 2.11 Ga. The average of $^{207}Pb/^{206}Pb$ ages for the 15 concordant data is 2075 ± 12 Ma (MSWD = 0.51). This is interpreted as the age of the granulite facies metamorphism.

3.4.4. Zircon ID05 (TT2)

We also observed two types of zircons in sample ID05: magmatic, which were dated at 2675 ± 11 Ma and metamorphic dated at 2080 ± 21 Ma by LA-ICPMS. In more detail, the first batch (1) is mainly composed of large elongate brown grains with "cores" or inner parts (grain 9, Fig. 10), which are U-poor (aver. 185 ppm) with brown zoned rims; some grains exhibit clear and U-rich overgrowths (spot 5.1 in Table 3). The second batch (2) is composed of euhedral clear grains (grains 8 & 17, Fig. 10) without cores, some of which are very U-rich (2134 ppm: grain 8.1, Table 3), whereas some of the others are U-poor (132 ppm: grain 17). Ages of the cores from set (1) are concordant to slightly discordant and $^{207}Pb/^{206}Pb$ ages range between 2.58 and 2.70 Ga for a set of 15 analyses (out of 20), which define an average at 2675 ± 11 Ma (MSWD = 0.68). This is interpreted as the age of the tonalitic precursor. One analysis from a clear overgrowth and three from euhedral clear grains from batch (2) give a $^{207}Pb/^{206}Pb$ average age of 2080 ± 21 Ma (MSWD = 0.19) interpreted as the age of the high grade metamorphic event.

3.4.5. Zircon 229-22 (TT5)

Zircon grains from sample 229-22 are also complex with cores dated by SHRIMP up to 2.7–2.9 Ga and metamorphic growths at 2098 ± 11 Ma. (Figs. 11 and 12). In more detail, the cores are elongate (gr. 6, 12 Figs. 11 and 12) to rounded (gr. 11, Fig. 11). They are generally zoned and U-rich (average around 800 ppm), with the exception of grain 16 (Table 2). They are interpreted as magmatic zircons. U–Pb ages for these cores are concordant to slightly discordant (Fig. 11, Table 2) and they range along the concordia curve between 2.3 Ga (16.2) and 2.9 Ga (11.2). They may correspond to several zircon generations or might result from lead loss during the high grade metamorphism. In that case the spread of data along the concordia would correspond to a discordia between the precursor and high grade metamorphism (more or less disturbed but late lead losses, Fig. 11): the tonalitic protolith may have formed ca 2.9 Ga. Alternatively, if the protolith is considered to have been formed ca 2.7 Ga, the 2.9 Ga age would indicate an inheritage process. Regardless of whatever the right interpretation might be, this sample contains Archaean zircons up to 2.7 and 2.9 Ga.

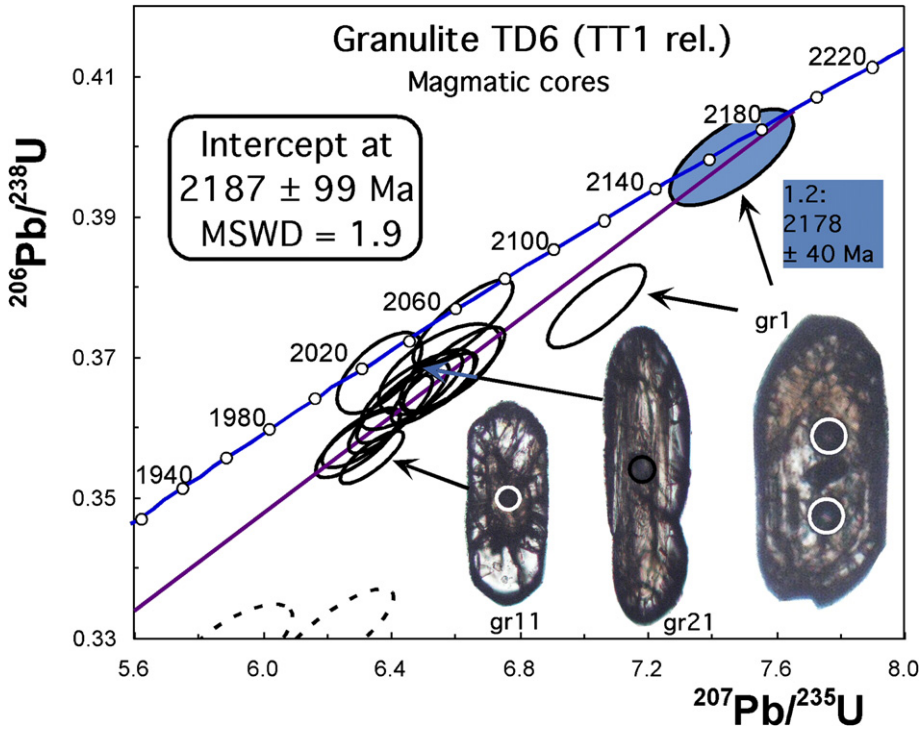

Fig. 8. Concordia diagram and TL images for magmatic zircons from granulite TD6 (TT1 rel.). LA-ICPMS analyses, ellipses are reported at 1σ. Spot size: 20 μm.

Clear round grains (gr. 9 and 15, Fig. 12) and overgrowths (gr. 1 and 12) are generally U-poor (average 126 ppm). Some grains are much depleted and exhibit high common lead content, which induces large errors on the ages (i.e. gr. 9, $U = 20$ ppm, Table 2). These low-U zircons are interpreted as metamorphic grains. The whole set of metamorphic zircons is concordant to slightly discordant and defines an average $^{207}Pb/^{206}Pb$ age of 2098 ± 11 Ma (10 analyses, MSWD = 1.2). One grain (7.2) is U-rich (2231 ppm) with a similar concordant age at 2097 ± 6 Ma, thus it is included in the calculation. The age of 2098 ± 11 Ma is interpreted as that of the granulite facies metamorphism.

3.4.6. *Metamorphic zircons*

In these granulites, metamorphic zircons are generally developed as clear overgrowths around elongated and rounded dark

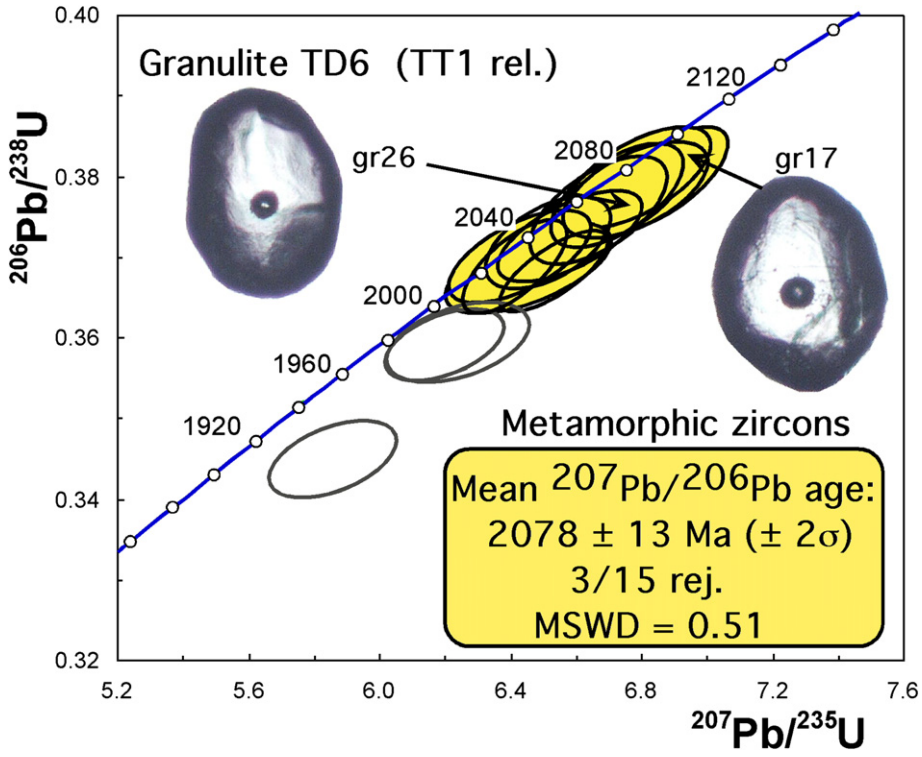

Fig. 9. Concordia diagram and TL images for metamorphic zircons from granulite TD6 (TT1 rel.). LA-ICPMS analyses, ellipses are reported at 1σ. Spot size: 20 μm.

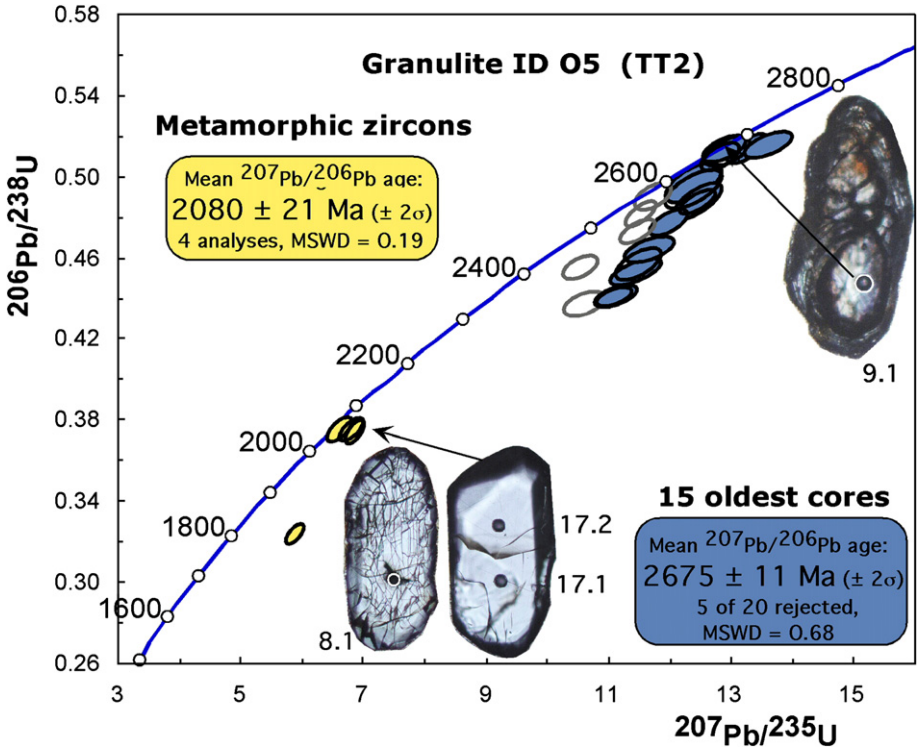

Fig. 10. Concordia diagram and TL images for magmatic and metamorphic zircons from granulite ID05 (TT2). LA-ICPMS analyses, ellipses are reported at 1σ. Spot size: 20 μm.

cores. They often exhibit an irregular zoning and are U-depleted compared to the cores, which show concentric zoning and are U-rich. Overgrowths can be strongly developed and can form metamorphic grains, which are generally clear and round (Figs. 9 and 11). In one sample (ID05, Fig. 10, Table 3), the metamorphic overgrowths are U-rich and synchronous with euhedral clear grains. They are all interpreted as related to the granulite facies metamorhism.

Metamorphic zircons from this area provide ages ranging between 2069 ± 19 Ma (Silva et al., 2002) and 2098 ± 11 Ma, the

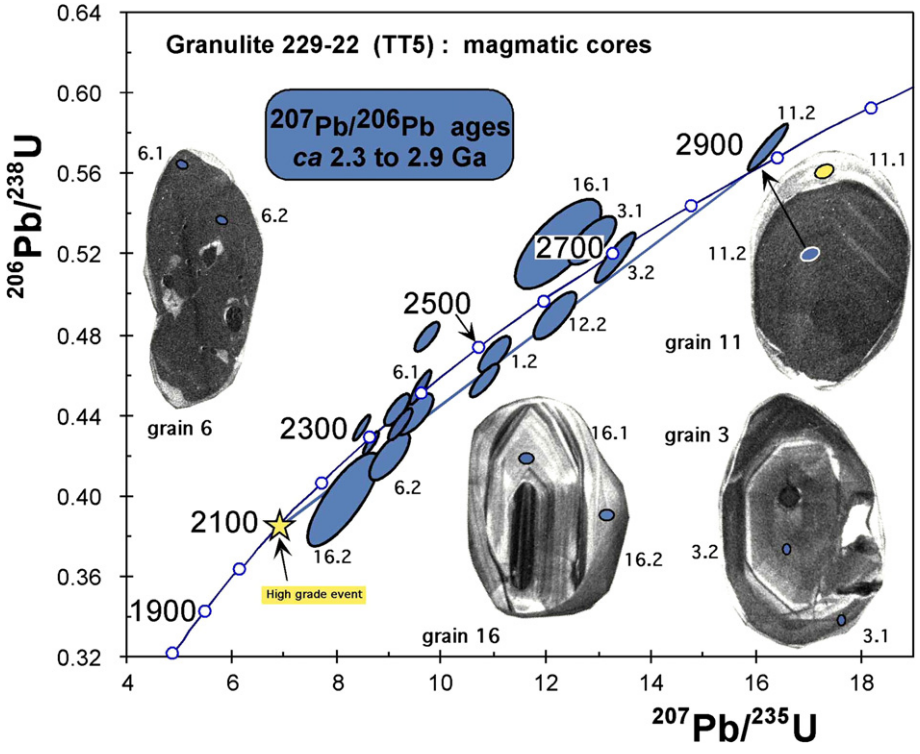

Fig. 11. Concordia diagram and CL images for magmatic zircons from granulite 229-22 (TT5). SHRIMP analyses, ellipses are reported at 1σ. Spot size: 30 μm.

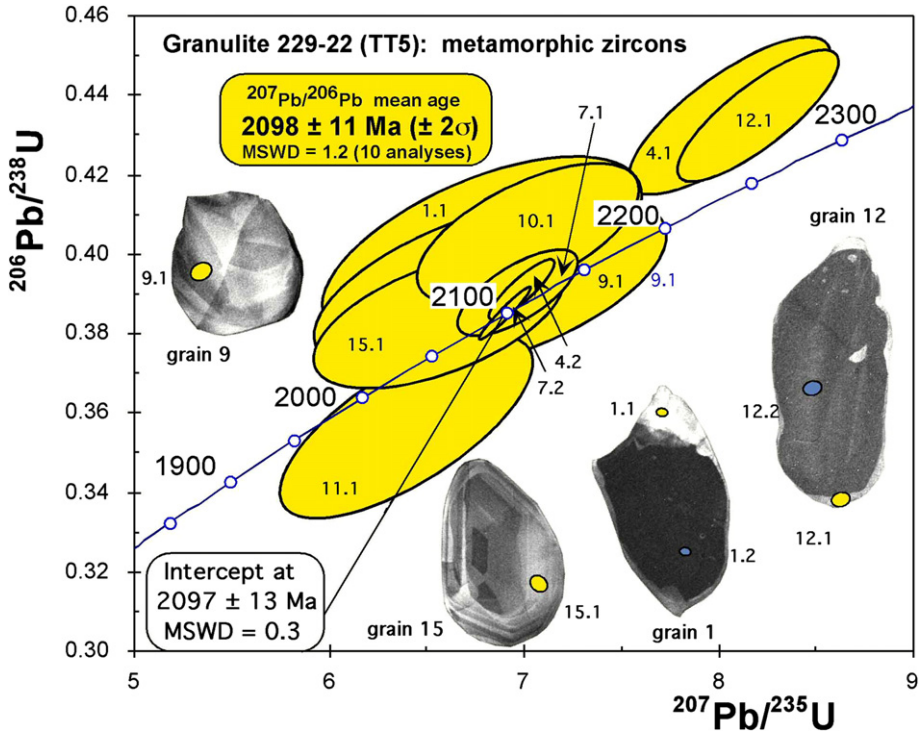

Fig. 12. Concordia diagram and CL images for metamorphic zircons from granulite 229-22 (TT5). SHRIMP analyses, ellipses are reported at 1σ. Spot size: 30 μm.

oldest age obtained in this work. On the other hand, the five sets of metamorphic zircons measured in this work gave $^{207}Pb/^{206}Pb$ ages that are not significantly different from each other, when taking the 2σ errors into account. The whole set of concordant to sub-concordant zircons (44 analyses with concordancy degree ≥ 90%, Fig. 13) results in an average $^{207}Pb/^{206}Pb$ age of 2086 ± 7 Ma (MSWD = 0.97), the gaussian-like distribution (Fig. 13) indicates that the spread is mainly related to error measurements. The result is considered to be the mean age for the granulite facies metamorphism in this part of the ISCB. The inclusion of data from Ledru et al. (1994) and Silva et al. (2002) in the calculation results in a similar average of 2087 ± 11 Ma (MSWD = 2.6, Table 4).

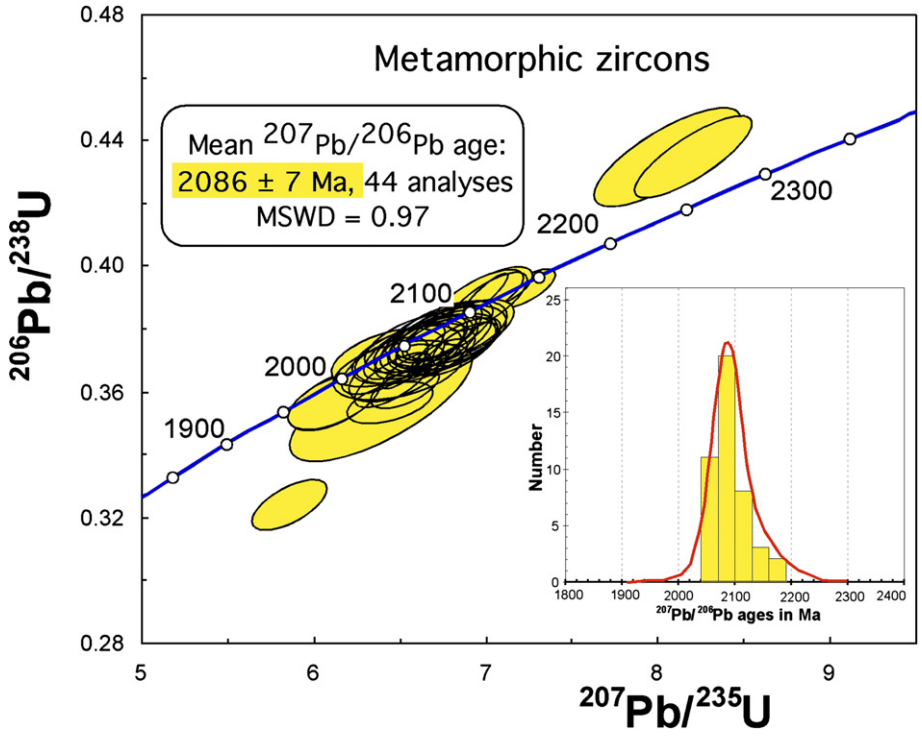

Fig. 13. Concordia diagram and histogram of $^{207}Pb/^{206}Pb$ ages for the whole set of metamorphic zircons obtained from the 5 samples of granulites (ellipses are reported at 1σ).

Table 4
Summary of zircon and monazite ages for the ISCB and the Jequié block.

Location protoliths	Sample	Rock type	Magmatic zircon age ± 2σ (inheritage)	Metamorphic age in Ma, ± 2σ	Metamorphic mineral dated	Methodology	Reference
Southern ISCB							
		alkaline suites:					
Palaeoproterozoic syn-granulitic	JQ5 granulite	shoshonitic	2075 ± 16[a] Ma	–		TIMS evap.	Ledru et al. (1994)
alk. magmas	JF35A K-rich granulite	shoshonitic	2089 ± 2	–	–	TIMS-ID	Alibert pers. com.
	Syenite of Sao Felix	syenite	2098 ± 1	–	zircon	TIMS evap	Rosa et al. (2001)
		calc-alkaline suites:					
Palaeoproterozoic syn-granulitic suites	LC50 granulite	charno-enderbite (TT1)	2092 ± 6	–	–	SHRIMP	Silva et al. (2002)
	YJ16 granulite	enderbite (TT1)	2109 ± 19	2081 ± 16	zircon	LA-ICPMS	this work
Palaeoproterozoic pre-granulitic	JM142A gneiss	tonalitic	2124 ± 10	–	–	SHRIMP	Silva et al. (2002)
calc-alkaline suites	LC51 granulite	enderbite TT1	2131 ± 5	2069 ± 19	zircon	SHRIMP	Silva et al. (2002)
	TD6 granulite	TT1 related	ca 2.18 Ga	2078 ± 13	zircon	LA-ICPMS	this work
	JF142A granulite	TT1	2191 ± 10	2109 ± 17	zircon	SHRIMP	this work
Archaean protoliths	JQ9 granulite	charno-enderbite	ca 2.5 Ga	2086 ± 36	zircon	TIMS evap.	Ledru et al. (1994)
	JQ 41 SW Ipiau	enderbite	2634 ± 14	–	–	TIMS evap.	Ledru et al. (1994)
	ID05 granulite	enderbite (TT2)	2675 ± 11	2080 ± 21	zircon	LA-ICPMS	this work
	LC 54 granulite	enderbite (TT2-TT5)	2719 ± 10	–	–	SHRIMP	Silva et al. (2002)
	LC 57 granulite	charno-enderbite	ca 2.85 Ga	2078 ± 20	zircon	SHRIMP	Silva et al. (2002)
	229-22 granulite	TT5	ca 2.7–2.9 Ga	2098 ± 11	zircon	SHRIMP	this work
average for metamorphic zirons/ S-ISCB: 2089 ± 10 M a (8 ages), MSWD = 2.2							
Central ISCB							
		alkaline suites:					
Palaeoproterozoic post-granulitic magmas	AM12A granite (Bravo)	granite	2063 ± 6		–	SHRIMP	Barbosa et al. (2008)
		calc-alkaline suites:					
Palaeoproterozoic syn to	LH182 granulite (Tanquinho)	charnockite	2096 ± 3	–	–	TIMS evap.	Barbosa et al. (2008)
pre-granulite magmas	AM05 granulite (Bravo)	enderbite	2070 ± 3	–	–	SHRIMP	Barbosa et al. (2008)
	CPRM7 Jacuipe/Casanova charnockite	2126 ± 19	2082 ± 7		zircon	SHRIMP	Silva et al. (1997)
	LH 55 orthogneiss (Conde)	granitic	2169 ± 48 (discordant)	–	–	SHRIMP	Silva et al. (2002)
Archaean protoliths	CPRM 9 Salvador City granulite	enderbite	2561 ± 7	2089 ± 11	zircon	SHRIMP	Silva et al. (1997)
	3.4 S.J. Jacuipe	leucograbbro	2584 ± 8	2082 ± 17	zircon	SHRIMP	Oliveira et al. (2010)
	CPRM8 S.J. Jacuipe town	charnockite	2634 ± 19 Ma (3.3 Ga)	2072 ± 22	zircon	SHRIMP	Silva et al., 1997
	CPRM6 S.J. Jacuipe dam	Opx tonalite	2695 ± 12 Ma	2072 ± 15	zircon	SHRIMP	Silva et al., 1997
	LR02 granulite (Riachao de Jacuip)	enderbite	ca 2.2 (ca 2.8 Ga[a])	2028 ± 13	zircon	SHRIMP	Silva et al. (2002)
	LR03 granulite (Capelinha)	enderbite	ca 2.6 Ga	–	–	SHRIMP	Silva et al. (2002)
	LH44 orthogneiss (Apora)	granodioritic	2954 ± 25	–	–	SHRIMP	Silva et al. (2002)
average for metamorphic zircons/ C-ISCB: 2082 ± 5 M a (6 ages), MSWD = 1.05							
Northern ISCB							
Palaeoproterozoic alk. suite:	Itiuba syenite	syenite	2084 ± 9	–	–	SHRIMP	Oliveira et al. (2004)
syn- to late-granulite magmas	Itiuba syenite	syenite	2095 ± 5	–	zircon	TIMS evap	Conceição et al., (2003)
Mafic & U.B.	Medrado high grade complex	gabbro-norite	2085 ± 5	–	–	SHRIMP	Oliveira et al. (2004)
Supracrustal belt	Caldearo belt	quartzite	(ca 2.7–3.2 Ga)	2076 ± 10	zircon (rims)	SHRIMP	Oliveira et al. (2002)
Archaean protoliths	PO 29.2 Caraiba granulite	noritic	2580 ± 10	2103 ± 23	zircon	SHRIMP	Oliveira et al. (2004)
	Caraiba airport	amphibolite	2577 ± 110	2083 ± 4	zircon	TIMS	D'el-Rey Silva et al., (2007)
	G2 granulite	tonalitic	2574 ± 6	2074 ± 14	zircon	SHRIMP	Oliveira et al., (2010)
average for metamorphic zircons/ N-ISCB: 2082 ± 8 (4 ages), MSWD = 2.1							
average for metamorphic zircons/ all ISCB: 2083 ± 4 M a (17 ages), MSWD = 1.9							

Jequié block							
Palaeoprot. syn-granulite melt	BJ137 gt-cord granulite Brejos	charnockite	–	2052 ± 14	monazite	TIMS evap.	Barbosa et al. (2004)
Archaean protoliths	CH2 Mutuipe	enderbite	2689 ± 7	–	–	SHRIMP	Alibert and Barbosa (1992)
	CH1 Jequiriä	charnockite	ca 2.8 Ga	–	–	SHRIMP	Alibert and Barbosa (1992)
	JQ 35 Valentino	charno-enderbite	2645 ± 20[a]	–	–	TIMS evap.	Ledru et al. (1994)
	LC 61 Jequié	charnockite	ca 2.5 Ga	2061 ± 6	zircon	SHRIMP	Silva et al. (2002)
	LC 60 Jitauna	charnockite	ca 2.7 Ga	2047 ± 14	zircon	SHRIMP	Silva et al. (2002)
	LC 62A	Ipiau charnockite	ca 2.6–2.8 Ga	2052 ± 16	zircon	SHRIMP	Silva et al. (2002)
	Brejos granulites	various charnockites	ca 2.6 Ga	–	–	TIMS evap.	Barbosa et al. (2004)
	PJ07 granulite of Brejos	charnockite	–	2047 ± 12	monazite	TIMS evap.	Barbosa et al. (2004)
average Jequié 2056 ± 9 Ma (5 ages), M SWD = 1.8							

[a] Re-interpreted age.

4. Discussion and conclusion

The occurrence of two main chronologic sets of granulites in this part of the ISCB, one Archaean and the other Palaeoproterozoic, is well constrained by the U–Pb zircon ages and Nd isotopic signatures. These two sets are also correlated to the chemical composition of the granulites (Barbosa and Sabaté, 2002; Pinho, 2005 and Pinho et al., 2011). When combining this chronological data set with geological mapping (Fig. 2), it appears that approximately 50% of the protoliths (tonalitic suites TT2 and TT5) are Archaean in age in the southern part of the ISCB. Consequently, this Archaean tonalitic crust appears to be a major component of the southern ISCB. Until now, the Archaean tonalitic crust in this area was classically considered as being subordinate relicts within Palaeoproterozoic plutons. Our work showed that the Archaean tonalitic crust is a main component of the southern ISCB.

Furthermore, these Archaean tonalitic-trondhjemitic suites display Nd signatures and U–Pb zircon ages identical to those measured in the Jequié granulites (ref. in geological setting). This is also true in the central ISCB (at the latitude of the Salvador city) with protoliths dated at ca 2.6, 2.7 and 2.9 Ga (Silva et al., 1997, 2002) and around 2.6 Ga further north (Oliveira et al., 2004, 2010) (Table 4). This indicates that the Palaeoproterozoic suites of the ISCB were emplaced on the eastern side of the Archaean Jequié-type terrains as previously proposed by Barbosa and Sabaté (2004).

The Palaeoproterozoic felsic granulites constitute two major groups, (1) the low-K calc-alkaline suites and (2) the shoshonitic to monzonitic ones. Group (1) provides zircon ages between 2131 ± 5 Ma (Silva et al., 2002) up to 2191 ± 10 Ma (this work). They are considered as emplaced (at least partially) before the high grade event (Pinho et al., 2011) and can be related to an active margin setting where juvenile crust was emplaced in the Jequié Archaean craton between 2.2 and 2.1 Ga. Both field relationships and zircon dating show that the alkaline suites (2) were emplaced later (Barbosa and Sabaté, 2004). Indeed, these rocks provided one TIMS zircon evaporation age at 2075 ± 16 Ma (Table 4, Ledru et al., 1994) and a second age at 2089 ± 2 Ma, as measured by the classical TIMS-ID method (Table 4, Alibert, pers. com.). The age of this alkaline magmatism is in the same range as the ages of the granulite facies metamorphism and is probably related to crustal thickening processes.

This work establishes a mean age of the granulite facies metamorphism for the southern ISCB at 2086 ± 7 Ma and at 2087 ± 11 Ma when data from the literature are included (data and references in Table 4). In the central part of ISCB, a set of six SHRIMP analyses of metamorphic zircons gives an average of 2082 ± 5 Ma for the age of the granulite facies metamorphism while in the northern ISCB, three SHRIMP and one TIMS ages of metamorphic zircons are also in the same range (Table 4). These data show that the high grade metamorphic event took place at the same time throughout the entire ISCB. Using all the ISCB in-situ zircon metamorphic ages (17 dates), we calculated a weighted average age of 2083 ± 5 Ma (MSWD = 2.1). In addition, and within the same time period, several large syenite massifs were emplaced in the São Francisco Craton like the Itiúba (2084 ± 9 Ma, Oliveira et al., 2004) and São Felix (2098 ± 1 Ma, Rosa et al., 2001) massifs. These massifs did not undergo granulite facies metamorphism, probably due to the fact that they were emplaced in medium crustal levels (Barbosa et al., 2004) or alternatively because they remained as closed systems during granulite facies metamorphism.

SHRIMP metamorphic zircon ages (Silva et al., 2002) and TIMS monazite ages (Barbosa et al., 2004) in the granulitic Jequié block are significantly younger that those of the ISCB with a weighted average of the $^{207}Pb/^{206}Pb$ ages at 2056 ± 9 Ma (Table 4). This age, which is in the range of that of the post-granulitic Bravo granite,

suggests a migration of crustal thickening processes towards the west when the ISCB uplifted on the east. Alternatively, Barbosa et al., (2004) interpreted these ages as reflecting late over-thrusting during the collision between the Jequié and Gavião blocks.

These geochronological data are perfectly consistent with the geodynamic model presented by Barbosa and Sabaté (2004) and also with that presented by Oliveira et al. (2010) for the northern ISCB. (1) A tholeiitic basaltic oceanic crust was subducted under the Jequié block between 2.2 and 2.1 Ga and then transformed into amphibolite and melted, thus generating orogenic calc-alkaline suites (TT1); they were emplaced in an active margin formed by Jequié-type Archaean rocks. We interpret the ISCB as the deep roots of the active margin characterised by imbrications of Archaean and Palaeoproterozoic tonalitic precursors. (2) The collision resulted in major crustal thickening in the ISCB mainly between 2.10 and 2.07 Ga and led to granulite facies metamorphic conditions at a temperature up to 1000 C and pressure up to 9 kb (Pinho, 2005), giving rise to syn-granulitic alkaline magmatism. The thrusting of the ISCB over the Jequié Block continued up to ca 2.05 Ga.

Acknowledgements

Thanks are due to CAPES, CNPq and COFECUB for financial supports and to CBPM for logistic support. C. Alibert is thanked for providing the U–Pb age of a shoshonitic granulite obtained by TIMS in the CRPG (Nancy, France). The collaboration between the graduation course in Geology and the Geophysics and Geology Research Centre of the UFBA is gratefully acknowledged. We also thank Dc S. Mullin who improved the final english version. We gratefully achnowledge the constructive reviews of two anonymous reviewers which helped to improve substantially the quality of the paper.

References

Alibert, C., Barbosa, J.S.F., 1992. In: Ages U–Pb déterminés à la SHRIMP sur des zircons du complexe de Jequié, Craton de São Francisco, Bahia, Brésil. Abstract, in 14è Réunion des Sciences de la Terre. Société Géologique de France, Toulouse, p. 4.

Alkmim, F.F., Brito Neves, B.B., Castro Alves, J.A., 1993. In: Dominguez, J.M.L., Misi, A. (Eds.), Arcabouço tectônico do cráton do São Francisco: uma revisão, pp. 45–62. O cráton do São Francisco. Salvador: SBG, SGM, CNPq.

Alves da Silva, F.C., 1994. Etude structurale de la greenstone-belt Paléoproterozoique du Rio Itapicuru (Bahia, Bresil). Thèse de l'Université d'Orléans, Orléans, France, 307 pp.

Barbosa, J.S.F., 1986. Constitution lithologique et métamorphique de la région granulitique du sud de Bahia-Brésil. Thèse de l' Université Pierre et Marie Curie, Paris, France, 401 pp.

Barbosa, J.S.F., 1990. The granulites of the Jequié complex and Atlantic mobile belt, southern Bahia, Brazil: an expression of archean-proterozoic plate convergence. In: Vielzeuf, D., Vidal, P. (Eds.), Granulites and crustal evolution. Springer Verlag, pp. 195–221.

Barbosa, J.S.F., Sabaté, P., 2002. Geological Features and the Paleoproterozoic Collision of Four Archaen Crustal Segments of the São Francisco Cráton, Bahia, Brazil: A Synthesis, vol. 74–2. Anais da Academia Brasileira de Ciências. 343–359.

Barbosa, J.S.F., Sabaté, P., 2004. Archaen and paleoproterozoic crust of the São Francisco Bahia, Brazil: geodynamic features, vol. 133. Precambrian Research. 1–27.

Barbosa, J.S.F., Martin, H., Peucat, J.J., 2004. Paleoproterozoic dome forming structures related to granulite facies metamorphism. Jequié block, Bahia, Brazil. Precambrian Research 135, 105–131.

Barbosa, J.F.S., Peucat, J.J., Martin, H., da Silva, F.A., de Moraes, A.M., Corrêa-Gomes, L.C., Sabaté, P., Marinho, M.M., Fanning, C.M.F., 2008. Petrogenesis of the late-orogenic bravo granite and surrounding high-grade country rocks in the paleoproterozoic orogen of Itabuna-Salvador-Curaçá block, Bahia, Brazil. Precambrian Research 167, 35–52.

Bastos Leal, R.L., Cunha, J.C., Cordani, U.G., Texeira, W., Nutman, A.P., Leal, A.B.M., Macambira, J.B.M., 2003. SHRIMP U–Pb 207Pb/206Pb zircon dating and Nd isotopic signature of the Umburunas greenstone belts, Northern São Francisco cráton, Brazil: evidence for intraplate extensional tectonics between 3340-3150 Ma. Journal of South American Earth Sciences 15, 775–785.

Conceição, H., Rosa, M.L.S., Macambira, M.J.B., Scheller, T., Marinho, M.M., Rios, D.C., 2003. 2,09 Ga idade mímina da cristalização do Batólito Sienítico Itiúba: um problema para o posicionamento do clímax do metamorfismo granulítico (2,05-2,08 Ga) no Cinturão Móvel Salvador-Curaçá, Bahia. Revista Brasileira de Geociências 33 (3), 395–398.

Cordani, U.G., Sato, K., Nutman, A.N., 1999. Single zircon SHRIMP determination from Archean tonalitic rocks near Uauà, Bahia, Brazil. In: Proceedings II South American symposium on isotope geology, 27–30.

Cunha, J.C., Fróes, R.J.B., 1994. Komatiitos com textura "spinifex" do Greenstone Belt de Umburanas, Bahia Série Arquivos Abertos, 7. Salvador: CBPM, 29 p.

D'el-Rey Silva, L.J.H., Dantas, E.T., Teixeira, J.B.G., Laux, J.H., da Silva, M.G., 2007. U–Pb and Sm–Nd geochronology of amphibolites from the Curaçá belt, São Francisco Craton, Brazil: tectonic implications. Gondwana Research 12, 454–467.

Hurai, V., Paquette, J.L, Huraiová, M., Konečný, P., 2010. Age of deep crustal magmatic chambers in the intra-Carpathian back-arc basin inferred from LA-ICPMS U-Th-Pb dating of zircon and monazite from igneous xenoliths in alkali basalts. Journal of Volcanology and Geothermal Research 198, 275–287.

Ledru, P., Johan, V., Milési, J.P., Tegyey, M., 1994. Markers of the last stages of the paleoproterozoic collision: evidence for a 2 Ga continent involving circum–South Atlantic provinces. Precambrian Research 69, 169–191.

Ludwig, K.R., 2001. User's manual for isoplot/ex, version 2.49. A geochronological tools it for Microsoft Excel. Berkeley Geochronology Center Special Publication, Berkeley. no. 1.

Marinho, M.M., 1991. La séquence volcano-sédimentaire de Contendas Mirante et la bordure occidentale du Bloc de Jequié (craton du São Francisco, Brésil): un exemple de transition Archéen-Protérozoique Thèse de l' Université de Clermont Ferrand, France, 170 p.

Marinho, M.M., Vidal, Ph., Alibert, C., Barbosa, J.S.F., Sabaté, P., 1994. Geochronology of the Jequié-Itabuna Granulitic Belt and of the Contendas-Mirante Volcano-sedimentary Belt, vol. 17. Boletim de Instituto de Geociências, Universidade de São Paulo, Brazil, Special Publication. 73–96.

Martin, H., Sabaté, P., Peucat, J.J., Cunha, J.C., 1991. Un segment de croûte continentale d'âge Archéean ancien (3.4 milliards d'années): le Massif de Sete Voltas (Bahia-Brésil). Comptes Rendus de l' Académie des Sciences, Paris 313, Série II, 531–538.

Mascarenhas, J.F., Silva, E.F.A., 1994. Greenstone Belt de Mundo Novo: caracterização e implicações metalogenéticas e geotectônicas no Cráton do São Francisco Série Arquivos Abertos 5, Salvador: CBPM, 32 p.

Melo, E.F., Xavier, R.P., Mcnaughton, N.J., Fletcher, I., Hagemann, S., Lacerda, C.M.M., Oliveira, E.P., 2000. Age constraints of felsic intrusions, metamorphism, deformation and gold mineralization in the paleoproterozoic Rio Itapicuru greenstone belt, NE Bahia State, Brazil. In: International Geological Congress, 31. Abstracts vol. special symposium. Stable and radiogenic isotopes in metallogenesis. CD-ROM.

Nutman, A.P., Cordani, U.C., 1993. SHRIMP U–Pb zircon geochronology of archean granitoids from the Contendas-Mirante area of the São Francisco Craton, Bahia, Brazil. Precambrian Research 163, 179–188.

Oliveira, E.P., Lafon, J.M., Souza, Z.S., 1999. Archaen-Proterozoic transition in the Uauá Block, NE São Francisco Craton, Brazil: U–Pb, Pb–Pb and Nd isotope constraints. In: SBG, SNET, 7, 1999. Lençóis 1, 38–40.

Oliveira, E.P., Mello, E.F., McNaughton, N.J., 2002. Reconnaissance U–Pb geochronology of Precambrian quartzites from the Caldeirão belt and their basement, NE São Francisco Craton, Bahia, Brazil: implications for the early evolution of the Paleoproterozoic Itabuna-Salvador Curuçá orogen. Journal of South American Earth Sciences 15, 349–362.

Oliveira, E.P., Windley, B.F., McNaughton, N.J., Pimentel, M., Fletcher, I.R., 2004. Contrasting copper and chromium metallogenic evolution of terranes in the Palaeoproterozoic Itabuna-Salvador-Curaçá orogen, São Francisco Craton, Brazil: new zircon (SHRIMP) and Sm-Nd (model) ages and their significance for orogen-parallel escape tectonics. Precambrian Research 128, 143–165.

Oliveira, E.P., McNaughton, N.J., Armstrong, R., 2010. Mesoarchaean to palaeoproterozoic growth of the northern segment of the Itabuna-Salvador-Curaçà orogen, São Francisco Craton, Brazil. In: Kusky, T.M., Zhai, M.G., Xiao, W. (Eds.), The Evolving Continents: Understanding Processes of Continental Growth, vol. 38. Geological Society, London, Special Publications, pp. 263–286. doi:10.1144/SP338.13.

Oliveira, E.P., Souza, Z., McNaughton, N.J., Lafon, J.M., Costa, F.G., Figueiredo, A.M., 2011. The Rio Capim volcanic-plutonic-sedimentary belt, São Francisco Craton, Brazil: geological and isotopic evidence for oceanic arc accretion during palaeoproterozoic continental collision. Gondwana Research 19, 735–750.

Peucat, J.J., Ménot, R.P., Monnier, O., Fanning, C.M., 1999. The Terre Adélie basement in the Antarctica Shield: geological and isotopic evidence for a major 1.7 Ga thermal events: comparison with Gawler craton in south Australia. Precambrian Research 94, 205–224.

Peucat, J.J., Mascarenhas, J.F., Barbosa, J.S.F., de Souza, S.L., Marinho, M.M., Fanning, C.M., Leite, C.M.M., 2002. 3.3 Ga SHRIMP U–Pb zircon age of a felsic metavolcanic rock from the Mundo Novo greenstone belt in the São Francisco Craton, Bahia (NE Brazil). Journal of South American Earth Sciences 15, 363–373.

Peucat, J.J., Santos Pinto, M., Martin, H., Barbosa, J.S., Fanning M,.C. 2003. SHRIMP U–Pb zircon ages up to 3.4-3.5 Ga in Archean and Paleoproterozoic granitoids of the Gavião Block, São Francisco Craton, Bahia, Brazil. Short papers, IV South American symposium on isotope geology, 252–255.

Pinho, I.C.A., 2005. Geologia dos Metatonalitos/Metatrondhjemitos e Granulitos Básicos das Regiões de Camamu-Ubaitaba-Itabuna, Bahia. PhD thesis. Instituto de Geociências, Universidade Federal da Bahia, Salvador, Brasil, 163 p.

Pinho, I.C.A., Barbosa, J.F.S., Leal, A.B.M., Martin, H., Peucat, J.J., 2011. Geochemical modelling of the tonalitic and trondhjemitic granulites from the Itabuna-Salvador-Curaçá Block, Bahia, Brazil. Journal of South American Earth Sciences 31 (2–3), 312–323.

Rios, D.C., Conceição, H., Davis, D.W., Rosa, M.L.S., Marinho, M.M., 2005. Expansão do Magmatismo Granítico Pós-Orogênico no Núcleo Serrinha (Ne Bahia), Cráton do São Francisco: Idade U–Pb do Maciço Granítico Pedra Vermelha. Revista Brasileira Geociências 35 (3), 423–426.

Rios, D.C., Davis, D.W., Conceição, H., Rosa, M.L.S., Dickin, A.P., Davis, W.J., Marinho, M.M., Stern, R., 2008. 3.65-2.10 Ga history of crust formation from zircon geochronology and isotope geochemistry of the Quijingue and Euclides plutons, Serrinha nucleus, Brazil. Precambrian Research 167, 53–70.

Rios, D.C., Davis, D.W., Conceição, H., Rosa, M.L.S., Dickin, A.P., 2009. Geologic evolution of the Serrinha nucleus granite-greenstone terrane (NE Bahia, Brazil) constrained by U–Pb single zircon geochronology. Precambrian Research vol. 170, 175–201.

Rosa, M.de.L.da.S., Conceição, H., Macambira, M.J.B., Scheller, T., Martin, H., Bastos Leal, L.R., 2001. Idades Pb-Pb e assinatura isotópica Rb-Sr e Sm-Nd do magmatismo sieníticopaleoproterozoico no sul do Cinturão Móvel Salvador-Curaçá: Maciço Sienítico de São Felix, Bahia. Revista Brasileira de Geociências 31 (3), 397–400.

Santos Pinto, M.A., 1996. Le recyclage de la croûte continentale archéene: Exemple du bloc du Gavião-Bahia, Brésil. Mémoires de Géosciences Rennes 75, 193.

Santos Pinto, M., Peucat, J.J., Martin, H., Sabaté, P., 1998. Recycling of the archean continental crust; the case study of the Gavião block, Bahia, Brazil. Journal of South American Earth Sciences 11 (5), 487–498.

Silva, M.G., 1996. Seqüências Metassedimentares, vulcanossedimentares e Greenstone Belts do Arqueano e Proterozóico Inferior. In: Barbosa, J.S.F., Dominguez, J.M.L. (Eds.), Geologia da Bahia: texto explicativo para o mapa geológico ao milionésimo. SICM/SGM, Salvador, pp. 85–102.

Silva, L.C., Mcnaughton, N.P., Melo, R.C., Fletcher, I. R., 1997. U–Pb SHRIMP ages in the Itabuna-Caraíba TTG high-grade complex: the first window beyond the paleoproterozoic overprint of the eastern Jequié cráton, NE Brazil. In: International symposium on granites and associated mineralization (ISGAM). 1997, Abstracts, Salvador. 282–283.

Silva, L.C., Armstrong, R., Delgado, I.M., Pimentel, M., Arcanjo, J.B., Melo, R.C., Teixeira, L.R., Jost, H., Cardoso Filho, J.M., Pereira, L.H.M., 2002. Reavaliação da evolução geológica em terrenos Pré-cambrianos brasileiros com base em novos dados U–Pb SHRIMP, parte I: Limite centro-oriental do Cráton do São Francisco. Revista Brasileira de Geociências 32 (4), 501–502.

Steiger, R.H., Jäger, E., 1977. Subcommission on geochronology: convention of the use of decay constants in geo- and comoschronology. Earth Planet Science Letters 36, 359–362.

Teixeira, W., Sabaté, P., Barbosa, J., Noce, C.M., Carneiro, M.A., 2000. Archean and Paleoproterozoic tectonic evolution of the São Francisco Craton. In: Cordani, U.G., Milani, E.J., ThomasFilho, Campos, D.A. (Eds.), Tectonic Evolution of South America. 31st International Geological Congress, Rio de Janeiro, pp. 101–137.

Williams, I.S., 1998. U-Th-Pb geochronology by ion probe. In: McKibben, M.A., Shanks III, W.C., Ridley, W.I. (Eds.), Applications of microanalytical techniques to understanding mineralizing processes. Reviews in economic geology, 7, pp. 1–35.

Wilson, N., 1987. Combined Sm-Nd, Pb-Pb and Rb-Sr geochronology and isotope geochemistry in polymetamorphic precambrian terrains: examples from Bahia, Brazil and Channel island, U.K. Master, Oxford University, England, 150 p.